AD_____
(Leave blank)

Award Number:
W81XWH-09-2-0091

TITLE:
Military Vision Research Program

PRINCIPAL INVESTIGATOR:
Darlene A. Dartt, Ph.D.

CONTRACTING ORGANIZATION:
Schepens Eye Research Institute
Boston, MA 02114

REPORT DATE:
February 2011

TYPE OF REPORT:
Final

PREPARED FOR: U.S. Army Medical Research and Materiel Command
Fort Detrick, Maryland 21702-5012

DISTRIBUTION STATEMENT: (Check one)
√ Approved for public release; distribution unlimited

☐ Distribution limited to U.S. Government agencies only;
report contains proprietary information

The views, opinions and/or findings contained in this report are those of the author(s) and should not be construed as an official Department of the Army position, policy or decision unless so designated by other documentation.

REPORT DOCUMENTATION PAGE

Form Approved
OMB No. 0704-0188

1. REPORT DATE *(DD-MM-YYYY)*	**2. REPORT TYPE**	**3. DATES COVERED** *(From - To)*
February 28, 2011	Final	1 AUG 2009 - 31 JAN 2011

4. TITLE AND SUBTITLE

Military Vision Research Program

5a. CONTRACT NUMBER
W81XWH-09-2-0091

5b. GRANT NUMBER
W81XWH-09-2-0091

5c. PROGRAM ELEMENT NUMBER

Darlene A. Dartt

Email: Darlene.dartt@schepens.harvard.edu

5d. PROJECT NUMBER

5e. TASK NUMBER
1-11

5f. WORK UNIT NUMBER

7. PERFORMING ORGANIZATION NAME(S) AND ADDRESS(ES)

Schepens Eye Research
Institute
20 Staniford Street

8. PERFORMING ORGANIZATION REPORT NUMBER

9. SPONSORING / MONITORING AGENCY NAME(S) AND ADDRESS(ES)

USA Med Research & Materiel
820 Chandler Street
Fort Detrick, MD 201702

10. SPONSOR/MONITOR'S ACRONYM(S)

11. SPONSOR/MONITOR'S REPORT NUMBER(S)

12. DISTRIBUTION / AVAILABILITY STATEMENT

Approved for public release; distribution unlimited

13. SUPPLEMENTARY NOTES

14. ABSTRACT

EYE INJURIES HAVE INCREASED IN WARFARE OVER THE PAST 200 YEARS. IN THE CURRENT CONFLICT THE EYE IS PARTICULARLY VULNERABLE TO BLAST INJURY AS WELL AS TO ENVIRONMENTAL STRESS FROM THE CURRENT THEATERS OF OPERATION. FOR CLEAR VISION, THE ENTIRE VISUAL AXIS (TEARS, CORNEA, AQUEOUS HUMOR, LENS, VITREOUS, RETINA, AND OPTIC NERVE) MUST BE TRANSPARENT, INTACT, AND HEALTHY AND EACH PART OF THIS AXIS FUNCTIONAL. EACH OF THESE STRUCTURES HAS ITS PARTICULAR VULNERABILITIES. IN THE PRESENT PROPOSAL WE HAVE DESIGNED MULTIPLE PROJECTS TO INVESTIGATE THE SPECIAL VULNERABILITIES OF THE CORNEA, RETINA, OPTIC NERVE, AND BRAIN TO MECHANICAL, LASER, INFECTIOUS, AND ENVIRONMENTAL TRAUMA AND TO DEVISE MEANS TO PREVENT, DIAGNOSE, AND REPAIR THE SEQUELAE OF THESE TRAUMAS.

15. SUBJECT TERMS
injury, laser injury, infection, angiogenesis, stem cells, dry eye, cornea, inflammation, traumatic brain injury, pain receptors, immune response

16. SECURITY CLASSIFICATION OF:			**17. LIMITATION OF ABSTRACT**	**18. NUMBER OF PAGES**	**19a. NAME OF RESPONSIBLE PERSON**
a. REPORT	**b. ABSTRACT**	**c. THIS PAGE**			Darlene A. Dartt, Ph.D.
unclassified	unclassified	unclassified	unclassified	48	**19b. TELEPHONE NUMBER** *(include area code)* 617-912-0272

Table of Contents

Task 1
Michael S. Gilmore, Ph.D.
Title: Cellular Defenses Against *S. aureus* Keratitis.

INTRODUCTION:

Infectious keratitis is characterized by corneal inflammation and damage caused by replicating bacteria, fungi, or protozoa. These infections can progress rapidly with devastating consequences, including corneal scarring and loss of vision. The principal risk factors of keratitis include trauma, contact lens wear, and ocular surgery. The goal of this research is to identify new approaches for augmenting corneal defenses against infection with antibiotic resistant pathogens, like Staphylococcus aureus, in high risk battlefield environments.

BODY:

The rate of methicillin resistant (MRSA) and fluoroquinolone resistant *Staphylococcus aureus* isolated from cases of keratitis is increasing. Due to the emergence of drug resistance, the search for new antibacterial targets and lead compounds is urgently required. Wall teichoic acids (WTA) are anionic glycopolymers that are covalently attached to peptidoglycan matrix of many gram-positive bacteria. WTA accounts for 30 to 60 % of the total cell wall mass and has been implicated in a number of a roles critical to maintaining the overall integrity of the cell envelope. We therefore are beginning to investigate the role of WTAs in *S. aureus* infection, and targeting their biosynthesis as a possible new therapeutic approach.

In collaboration with its developer, using a second generation wall teichoic acid inhibitor[1], termed compound 4-89, we more rigorously tested eukaryotic tissue toxicity by examining the ability of the compound to stimulate release of haemoglobin from human erythrocytes over extended, high level exposure. As shown below, a low level toxicity emerges at high concentrations over extended times, indicating that the compound may not be appropriate for long term or high dose therapy, or that additional structural refinements need to be made.

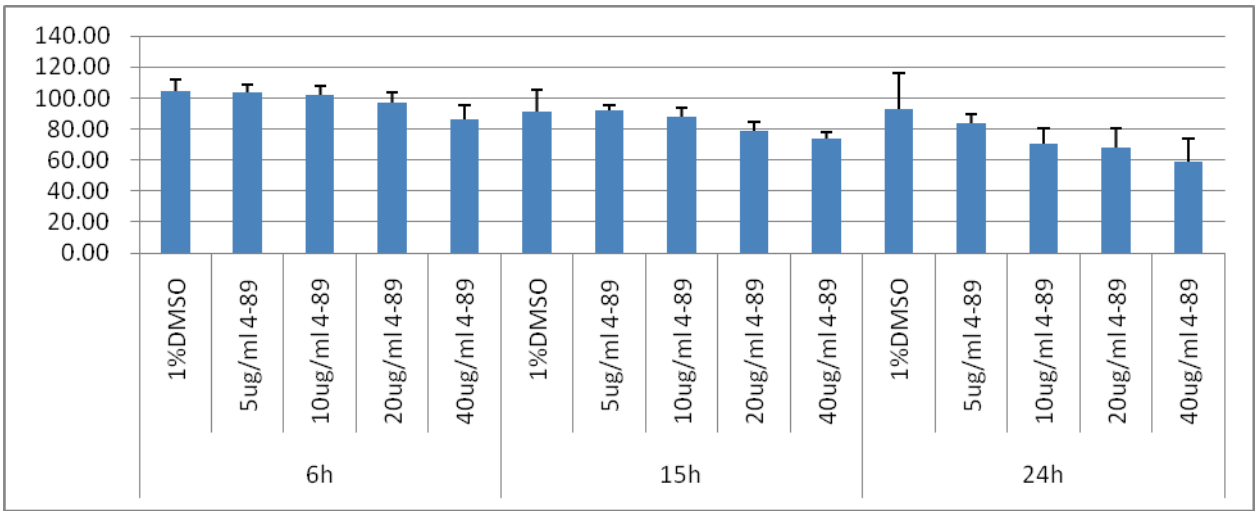

We also found that the presence of human corneal epithelial cells did not influence the efficacy of experimental compound 4-89 (or the vancomycin control [VCM]) against blood stream and keratitis isolates of *S. aureus* (Newman and MG2375 respectively, below).

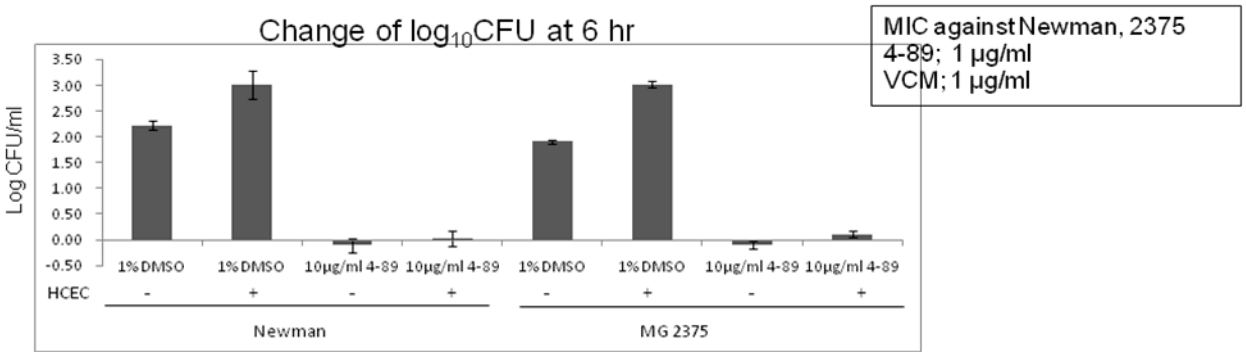

These results suggest that inhibitors of wall teichoic acid biosynthesis may represent excellent lead compounds for development of topical or systemic antibiotics. Low level toxicity as reflected by haemoglobin release indicates that additional refinement and testing is needed.

KEY RESEARCH ACCOMPLISHMENTS:

- Found that inhibitors of *S. aureus* WTAs possess a low level, dose responsive toxicity for erythrocytes over protracted time periods.
- Found that the drug is not inhibited, sequestered or metabolized in a manner that adversely affects its *S. aureus* inhibitory activity.

REPORTABLE OUTCOMES:

Heimer S, Yamada A, Russell H, and Gilmore MS. 2010. "Response of corneal epithelial cells to Staphylococcus aureus" In press.

CONCLUSION: Our results above demonstrate that the WTA biosynthesis pathway of *S. aureus* appears to be a viable target for preventing and treating keratitis caused by *S. aureus* strains, and that lead compound 4-89 has many of the ideal qualities of such a drug although additional refinement and testing is needed.

REFERENCES:

Development of improved inhibitors of wall teichoic acid biosynthesis with potent activity against *Staphylococcus aureus.* Lee K, Campbell J, Swoboda JG, Cuny GD, Walker S. Bioorg Med Chem Lett 2010; 20:1767-70.

Task 2

Darlene A. Dartt, Ph.D.

Title: Identification of Pain Receptors in Ophthalmic Trigeminal Nerves

INTRODUCTION:

Acute nociceptive pain, even though unpleasant, is a critical component of the body's defense system as a part of the warning relay to protect the eye from the environment and to warn about damage. The ocular surface, especially the cornea is densely innervated with sensory nerves that provide this function. The cornea contains nocieceptive nerve fibers that are activated by different types of stimuli that exclusively elicit the perception of pain. The cell bodies that give rise to the corneal sensory nerves originate in the ophthalmic branch of the trigeminal ganglion. The cells of the trigeminal ganglia contain the same pain receptors as the nerve endings. In the present study we propose to isolate the trigeminal ganglion cell bodies and study their transient receptor potential (TRP) pain receptors, especially TRPV1, TRPA1, and TRPM8. Activation of TRP receptors causes an influx of Ca^{2+} into the cell through the pain receptor ion channel. We are able to measure the intracellular [Ca^{2+}] by fluorescent microscopy. We will characterize the response of the different pain receptors on the ganglion cells and determine if the inflammatory mediator LTB_4 alters the Ca^{2+} response. We have the following objectives: 1) Isolate and culture trigeminal nerves; 2) Determine if functional TRV1, TRPA1, and TRPM8 pain receptors are present in trigeminal nerves; and 3) Determine if the inflammatory mediator LTB_4 increases the sensitivity of the TRV1, TRPA1, and TRPM8 pain receptors.

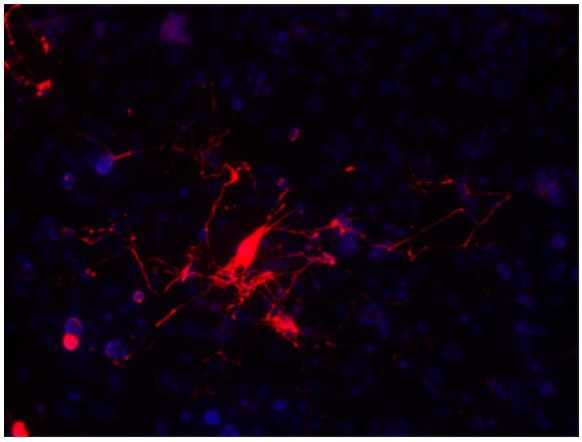

Figure 1. Cultured nerve cells expressing nerve growth factor are shown in red. Blue color indicates cell nuclei labeled with DAPI.

BODY

Objective 1: Isolate and culture trigeminal nerves. We have successfully isolated and cultured trigeminal nerve cells from rat. To isolate these cells, the trigeminal nerve was removed from rats and dissected into small pieces. The pieces were subjected to digestion with papain (40 U/ml), cysteine (0.6 mg/ml), and sodium carbonate (0.2 mg/ml) for 20 minutes at 37 °C. The dispersed tissue was centrifuged and resuspended in collagenase type II (3 mg/ml) and dispase type II (4 mg/ml) in Hank's balanced salt solution for 20 minutes at 37 °C. The cells were resuspended in L-15 media and layered over a percoll gradient (30-60%) and centrifuged at 2500 rpm for 20 minutes to separate nerve cells from blood cells. Nerve cells were layered again over 30% percoll and centrifuged at 750 rpm for 10 minutes. The cells were then resuspended in F12 media and plated on laminin-coated coverslips overnight. A mixed population of nerve and support cells was obtained. Trigeminal nerve and support cells on coverslips were fixed in 4%.paraformaldehyde for 4 hours at 4 °C. The cells were then subjected to immunofluorescence experiments using antibodies directed against neural cell markers for the nerve growth factor receptor p75, neurofilament 200 and nerve growth factor as well as DAPI, a marker for cell nuclei. Cultured trigeminal nerve cells express p75 and neurofilament 200 in both their cell bodies and processes. Similarly, cultured nerve cells also express nerve growth factor in their cell bodies and processes (Figure 1). Thus, we have successfully isolated and grown trigeminal nerve cells in culture.

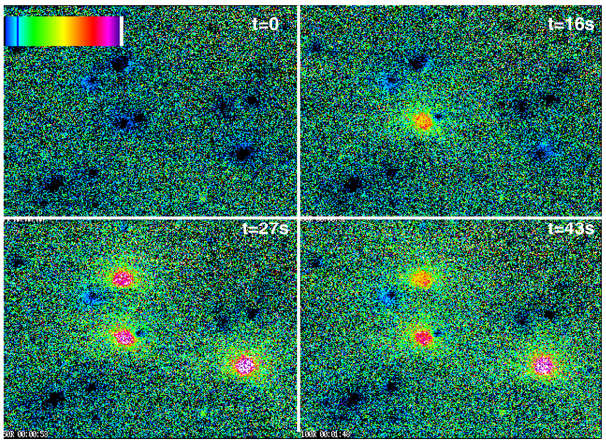

Figure 2. Capsaicin (10^{-8} M) increases intracellular [Ca^{2+}] in cultured trigeminal nerve cells. Cells were loaded with fura-2 for 1 h prior to addition of capsaicin. Intracellular [Ca^{2+}] was measured on Incyte Im2TM Ratio Imaging System using excitation wavelengths of 340 and 380 nm.

Objective 2) Determine if functional TRV1, TRPA1, and TRPM8 pain receptors are present in trigeminal nerves. Cultured trigeminal nerve cells were incubated with fura-2 ester, the fluorescent dye used to measure the intracellular [Ca^{2+}] and stimulated with 40 mM KCl that activates voltage-dependent ion channels that increase the intracellular [Ca^{2+}] independently of cell surface receptors. We found that 1 mM was the optimum fura-2 concentration to give a substantial and reproducible Ca^{2+} response to KCl. Capsaicin, an agonist for TRPV1 receptors was added to the fura-2 loaded trigeminal neurons (Fig 2). Capsaicin increased the intracellular [Ca^{2+}] in the neurons in a concentration-dependent manner with 10^{-6} M giving a maximum increase of about 380 nM (Fig 3 and 4). When the TRPV1 antagonist capsezepine (10^{-5} M) was added before capsaicin (10^{-6} M) the Ca^{2+} response was completely blocked. These data suggest that trigeminal neurons have a functional TRPV1 receptors that give a robust increase in intracellular [Ca^{2+}].

We next tried the TRPM8 agonist icillin. In four experiments, at 10^{-6}M icilin increased intracellular [Ca^{2+}] to 223 nM. At 10^{-5} M icillin [Ca^{2+}] was increased to 260 nM (Fig 5).

At the lower concentration of icillin 8% of the cells responded compared to the higher concentration at which 14% of cells responded. These data suggest that trigeminal neurons have functional TRPM8 receptors that increase the intracellular [Ca^{2+}].

Objective 3) Determine if the inflammatory mediator leukotriene (LT) LTB_4 increases the sensitivity of the TRV1, TRPA1, and TRPM8 pain receptors. Cultured trigeminal neurons were stimulated with capsaicin (10^{-6} M) followed by LTB_4 at 10^{-12} to 10^{-9} M. Capsaicin increased the intracellular [Ca^{2+}] to over 200 nM. No concentrations of LTB_4 altered the [Ca^{2+}] (Fig 6). Thus one of the leukotriene inflammatory mediators does not alter the TRPV1 response.

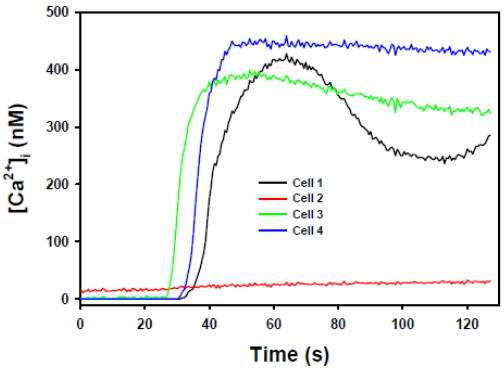

Figure 3. Capsaicin (10^{-8} M) increases intracellular [Ca^{2+}] in cultured trigeminal nerve cells. Cells were loaded with fura-2 for 1 h prior to addition of capsaicin. Intracellular [Ca^{2+}] was measured on Incyte Im2TM Ratio Imaging System using excitation wavelengths of 340 and 380 nm.

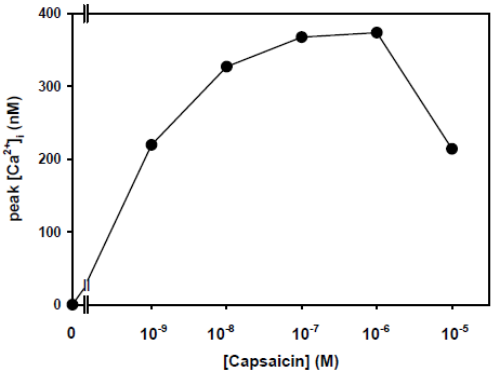

Figure 4. Capsaicin increases intracellular [Ca^{2+}] in cultured trigeminal nerve cells in a concentration-dependent manner.

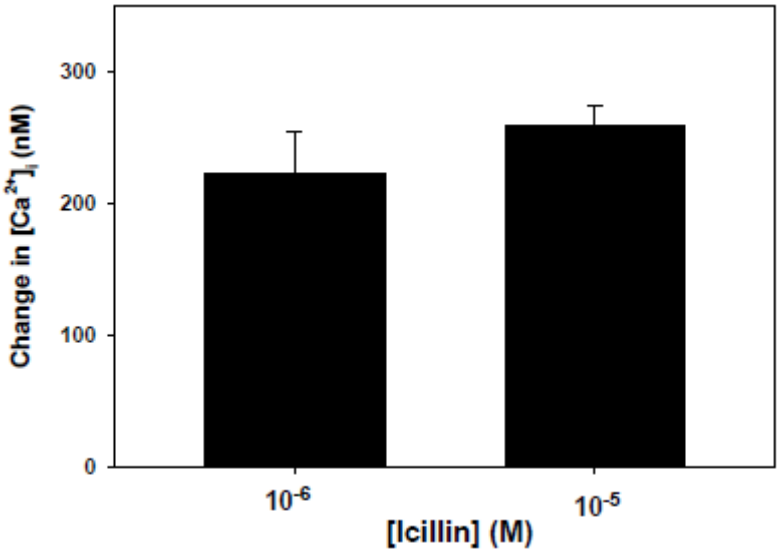

Figure 5. Icillin increases intracellular [Ca^{2+}]$_i$ in cultured trigeminal

nerve cells.

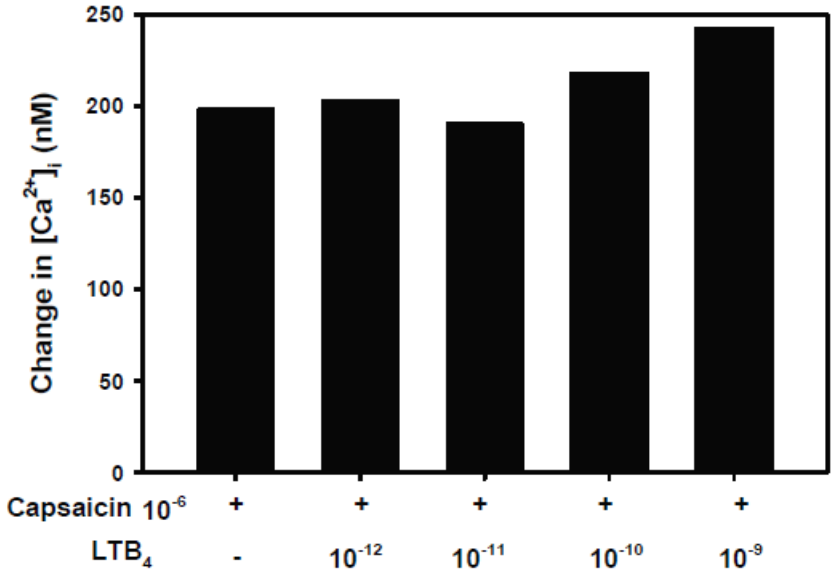

Figure 6. Leukotriene B_4 (LTB_4) does not affect capsaicin-induced increase in intracellular $[Ca^{2+}]_i$ in cultured trigeminal nerve cells.

Industry funding has been received to complete this project.

KEY RESEARCH ACCOMPLISHMENTS:

- Isolated and cultured trigeminal nerve cell bodies
- Identified nerve cell bodies
- Measured the intracellular $[Ca^{2+}]$ in cultured trigeminal nerve cell bodies
- Identified TRPV1 receptors on the cultured neurons.
- Identified TRPM8 receptors on the cultured neurons
- Found that a leukotriene inflammatory mediator does not alter the TRPV1 response

REPORTABLE OUTCOMES: None

CONCLUSION:

Trigeminal nerve cell bodies can be reproducibly isolated from the rat trigeminal ganglion and the nerve cell bodies identified in the mixed cell culture. Active TRPV1 and TRPM8 receptors are present on these nerve cell bodies. However, the inflammatory mediator chosen did not alter the TRPV1 response. We will continue to use these sensory nerve cells to determine if other pain receptors are present and if other inflammatory mediators on the ocular surface potentiate the pain response in injury and a variety of ocular surface diseases. The pain could be treated by designing drugs to block the activation of the pain receptors.

Task 3
Reza Dana, M.D., M.P.H., M.Sc.
Title: **Molecular regulation of corneal and ocular surface inflammation**

INTRODUCTION:
The cornea has the unique feature (except for the cartilage) of being normally avascular, but under many pathologic conditions vessels invade the cornea from the limbal vascular plexus. A wide variety of injuries, including infection, inflammation, ischemia, degeneration, trauma, and the loss of limbal stem cell barrier can cause corneal neovascularization (NV). Corneal NV not only frequently leads to corneal clouding, a leading cause of blindness, but also results in the loss of the immune privilege of the cornea, thereby worsening the prognosis of subsequent penetrating keratoplasty. Preexisting corneal stromal blood vessels have been identified as strong risk factors for immune rejection after corneal transplantation. For this reason, it is critical to understand the molecular and cellular mechanisms of corneal NV and inflammation.

BODY:
A novel group of lipid mediators, including aspirin-triggered lipoxin (ATL) and resolvins (RvD1 and RvE1) are actively produced during the resolution phase of inflammation to reestablish normal homeostasis. They reduce neutrophil trafficking, regulate reactive oxygen species, and display potent anti-inflammatory and immunoregulatory functions. In general, constant inflammation often leads to neovascularization in corneal diseases. Therefore, we hypothesized that ATL analog (ATLa), RvD1 and RvE1 inhibit inflammatory corneal angiogenesis via the suppression of innate immunity.

Chemokines play an important role in a number of physiologic and pathological inflammatory responses and are key regulators of leukocyte migration. In addition to the classical signaling chemokine receptors, a new subset of atypical chemokine receptors has emerged. This subfamily is characterized by the ability to internalize and degrade chemokine ligands but yet lack of signaling pathway. D6 receptor, one of the atypical chemokine receptors, actively scavenges inflammatory CC-chemokines and appears to play an essential role in the resolution on inflammatory responses.

The experiments that define this study are based on the following hypothesis: D6 chemokine decoy receptor can degrade a broad range of inflammatory chemokines and its expression on leukocytes and lymphatic endothelial cell limits the inflammatory response. To test this hypothesis, we plan to verify the functional relevance of D6 decoy receptor expressed by the cornea by comparing the degree of angiogenesis in mice lacking D6 decoy receptor gene with normal wild-type animals.

SPECIFIC AIMS:
1) Determine the functional relevance of recruited innate immune cells in new blood vessel formation.
2) Determine the ability of Lipoxin analogs to suppress vascular endothelial growth factor receptor-2 (VEGFR-2) and/or VEGFR-3-mediated angiogenesis and inflammatory cell recruitment.

3) Determine the expression and function of regulatory (decoy) mechanisms that could suppress corneal vascularization

- In the first experiment set, we determined the expression of the receptors of ATLa and RvE1in different portions of cornea tissue. As shown in **Figure 1**, we clearly identified that the receptors for LXA4, ALX/Fpr-rs-2, and for RvE1, ChemR23, were expressed by epithelium, stromal keratocytes and infiltrated $CD11b^+$ cells in corneas.

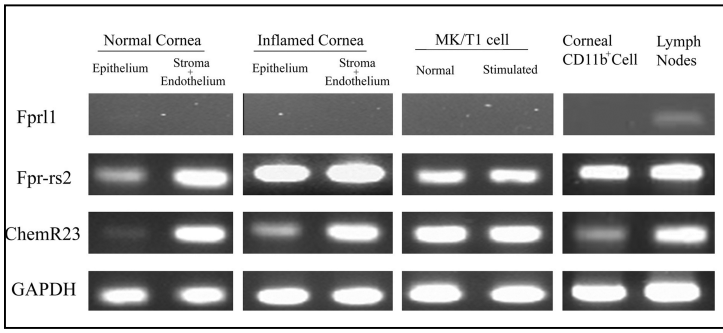

Figure 1. The expression of the receptors of LTA4 (Fprl1, Fpr-rs2) and RvE1 (ChemR23) in the epithelium, stromal-endothelium, MK/T-1 cells (corneal keratocyte cell line, with or without TNF-α and IL-1β stimulation) and FACS-sorted $CD11b^+$ cells from inflamed corneas, were determined using RT-PCR. Lymph nodes were used as positive controls.

- Next, we induced corneal angiogenesis by intrastromal sutures, then administrated ATLa, RvD1, or RvE1 subconjunctively to assess the effect of these lipid mediators on innate immune cell infiltration and inflammatory cytokine expression. In **Figure 2**, we showed a significant reduction in the number of infiltrated neutrophils (NIMP-$R14^+$ cells) and macrophages ($F4/80^+$ cells) and mRNA expression levels of IL-1β and TNF-α in the groups treated with lipid mediators, compared to the vehicle-treated group.

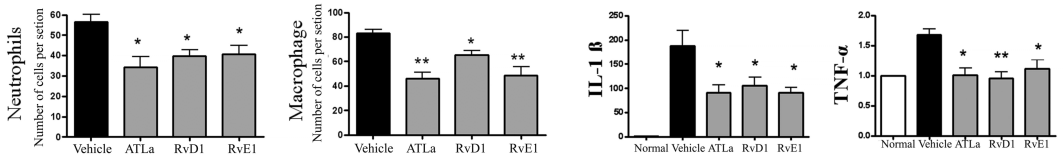

Figure 2. Subconjunctival administration of ATLa, RvD1, RvE1, significantly inhibited the infiltration of neutrophils (NIMP-$R14^+$ cells) and macrophages ($F4/80^+$ cells), and the mRNA expression levels of IL-1β and TNF-α after suture placement.

-

- Neovascularization is a common complication following inflammation. The anti-angiogenesis effect of ATLa has been reported previously. Here, we hypothesized that ATLa, RvD1 or RvE1 inhibit corneal inflammatory angiogenesis. First, we determined that treatments with ATLa, RvD1 or RvE1 significantly decrease the expression of VEGF-A, C and their receptor, VEGFR2, after suture placement (see **Figure 3 of appended manuscript**). Then, we evaluated corneal angiogenesis both intravitally and morphometrically. As show in **Figure 3**, application of any of the three lipid mediators led to significant suppression of hemangiogenesis, but not lymphangiognesis after intrastromal suture-placement.

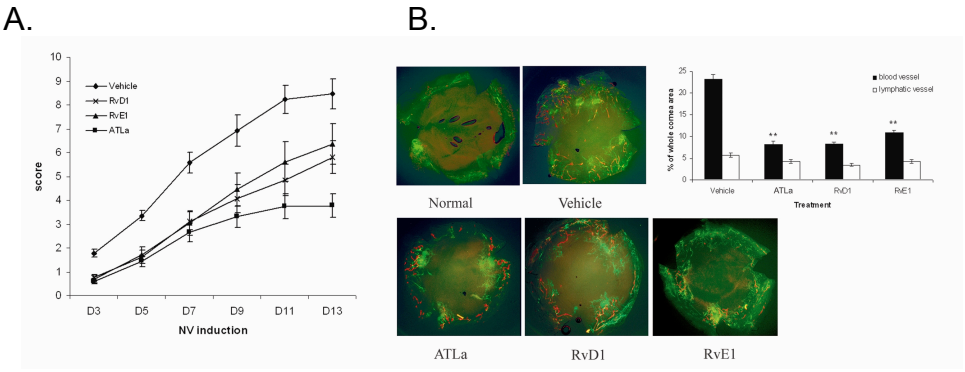

Figure 3. Subconjunctival administration of ATLa, RvD1, RvE1 has significantly reduced the corneal nevascularization during 2 week observation after suture placement **(A)**. On day 14, the density of blood vessels ($CD31^{high}/LYVE\text{-}1^{-}$) or lymphatic vessels ($CD31^{low}LYVE\text{-}1^{high}$) covering the cornea was measured after anti-CD31 (green) and anti-LYVE-1 (red) double staining **(B)**.

– To further analyze the direct regulatory effects of these lipid mediators on VEGF-A-induced angiogenesis versus a more 'indirect' inhibitory effect on angiogenesis via suppression of innate immune responses, we measured hemoangiogenesis and lymphangiogenesis after intrastromal placement of micropellets loaded with IL-1β or VEGF-A. As illustrated in **Figure 4**, ATLa, RvD1 and RvE1 significantly suppressed IL-1β-induced hemoangiogenesis, but not lymphangiogenesis. In addition, only ATLa-treatment significantly suppressed VEGF-A-induced hemoangiogenesis.

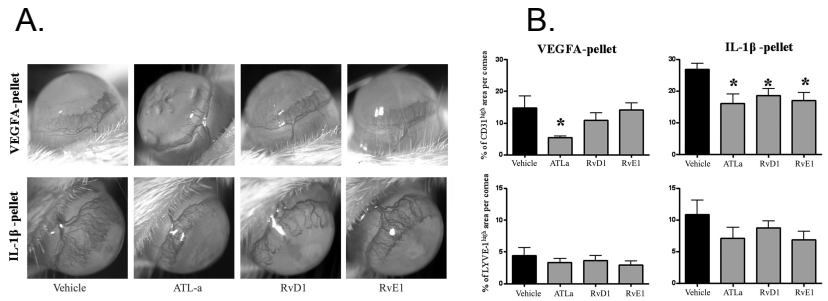

Figure 4. Corneal neovascularization of each treatment group was observed on day 7 via slip lamp biomicroscopy **(A)**. On day 7, the density of blood vessels ($CD31^{high}/LYVE\text{-}1^{-}$) or lymphatic vessels ($CD31^{low}LYVE\text{-}1^{high}$) covering the cornea was measured **(B)**.

– It had been shown that D6 is expressed by immune cells in addition to the lymphatic endothelial cells. However, the specific population of cells in which D6 is expressed had not been identified. In order to accomplish this we used flow cytometry to stain for macrophage (CD11-b), neutrophil (GR-1), T cell (CD4 and CD8) and DC (CD11c) markers and double stained with D6 antibody. As illustrated in **Figure 5**, we clearly identified that DCs express a higher level of D6 compared to other immune cells.

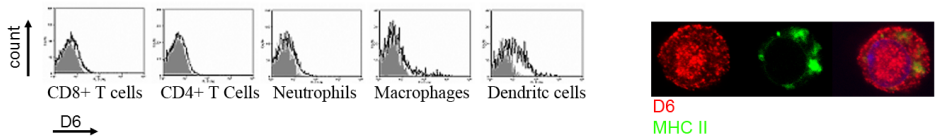

Figure 5. DCs highly express D6. Leukocyte were isolated from either spleen or peripheral blood and stained for cell-specific markers and D6 using appropriate antibodies (CD8 or CD4: T cells; GR1+: Neutrophils; CD11b+: Macrophages; CD11c+: dendritic cells) and analyzed using flow cytometry. Double staniing of MHC II and D6 chemokine receptor in DC shows the expression of D6 by a mature DC.

– We had previously shown that DCs are infiltrating the cornea following inflammation. We hypothesized that D6 expression by DCs inhibits additional infiltration of DC to the cornea and reduces the inflammation. In order to identify the role of D6 expression in corneal inflammation we used a well-established cautery model and stained for DC infiltration in the cornea. As shown by the **Figure 6** more DC infiltrates to the cornea in D6 -/- mice compared to the wild type animal.

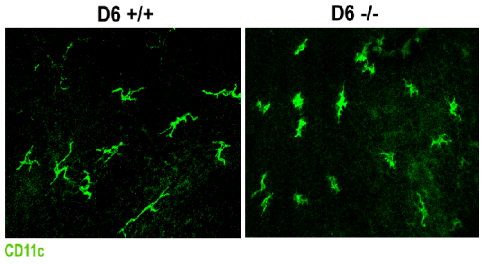

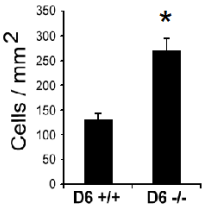

Figure 6.A larger number of dendritic cells infiltrate into the cornea following inflammation induced by cautery in D6 knockout mice.

– Following injury, inflammatory cells infiltrate into the cornea and act as a source of angiogenic factors. As inflammation is a key factor in corneal angiogenesis, we hypothesized that D6 expression plays a role in controlling inflammation and corneal angiogenesis. We evaluated the level of D6 expression in FGF induced angiogenesis and observed higher level of D6 expression on after FGF implantation. Consequently D6 -/- mice had significantly higher angiogenic response compared to wild type mice as shown in **Figure 7**.

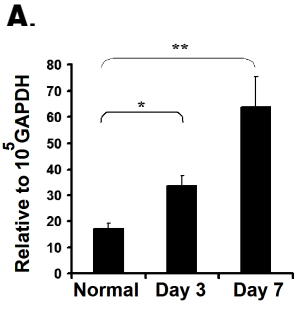

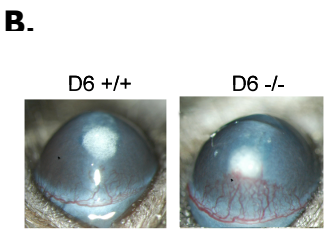

Figure 7. Angiogenesis is significantly higher in D6-/- mice. **A.** Corneal expression level of D6 chemokine receptor is increased after implantation of 40 ng b-FGF micropellet into the cornea. **B.** D6 knockout mice have higher angiogenic response to b-FGF micropellet compared to WT mice.

KEY RESEARCH ACCOMPLISHMENTS:

Aim 1:

- Our data suggest that signaling through VEGFR-3-specific ligands can induce NV and that macrophages contribute a significant role.

- Macrophages are present in VEGF-A-mediated angiogenesis and their depletion has the greatest inhibitory effect on VEGFR-3-mediated NV.

Aim 2:

- Corneal tissues and infiltrating innate immune cells express Fpr-rs2 (the LXA4 receptor) and ChemR23 (the RvE1 receptor).

- ATLa, RvD1, and RvE1 effectively resolve corneal inflammation and angiogenesis (hemoangiogenesis but not lymphangiogenesis) by controlling innate inflammation and marked reduction of pro-inflammatory cytokine secretion and inhibiting VEGF/VEGFR expression.

- ATLa has direct regulatory effect on angiogenesis but not through its anti-inflammatory effect.

Aim 3:

- Corneal dendritic cells express D6 chemokine receptor and infiltrate the cornea following inflammation. Lack of D6 expression results in greater number of inflammatory cells infiltrating the cornea. D6 expression by leukocytes controls corneal inflammation and knocking out D6 results in greater corneal angiogenesic responses to inflammatory stimuli.

REPORTABLE OUTCOMES:

1. Jin Y, Arita M, Zhang Q, Saban DR, Chauhan SK, Chiang N, Serhan CN, Dana R. Novel Anti-inflammatory and Pro-resolving Lipid Mediators Block Inflammatory Angiogenesis. *Invest Ophthalmol Vis Sci* 2009; 50(10):4743-52..

2. Hajrasouliha AR, Sadrai Z, Dana R. The role of chemokine decoy receptor D6 receptor on corneal inflammation and angiognesis. Poster Presentation at *The Association for Research in Vision and Ophthalmology (ARVO),* Fort Lauderdale, Florida, May 2010.

CONCLUSION:

The novel lipid mediators ATLa, RvD1, and RvE1 offer a potentially new therapeutic strategy for controlling corneal angiogenesis, a leading cause of blindness worldwide and a common complicating factor for ocular injuries suffered by military personnel. Our results support the importance of chemokine regulation through D6 in corneal angiogenesis and describe a new mechanism of immune modulation within the cornea.

APPENDIX:
Copy of manuscript based on work supported by grant is appended: Jin Y, Arita M, Zhang Q, Saban DR, Chauhan SK, Chiang N, Serhan CN, Dana R. Novel Anti-inflammatory and Pro-resolving Lipid Mediators Block Inflammatory Angiogenesis. *Invest Ophthalmol Vis Sci* 2009; 50(10):4743-52..

Task 4
Nancy Joyce, Ph.D.
Title: Use of Umbilical Cord Blood Mesenchymal Stem Cells to Repair Corneal Endothelium

INTRODUCTION:
Full-thickness transplantation of donor corneas (penetrating keratoplasty) has been used as the major means to restore vision to those who have sustained traumatic corneal injury. Unfortunately, the supply of healthy donor corneas is decreasing world-wide. As a result, researchers have been seeking new methods to treat corneal injuries, including corneal endothelial cell loss. One method involves transplantation of only the posterior portion of donor corneas, including Descemet's membrane and endothelium (DSEK, DLEK, DMEK)[1-3]. Another method is to use cultured donor corneal endothelial cells to develop bioengineered corneal constructs or equivalents[4-6]. Human corneal endothelial cells (HCEC) have a finite ability to divide[7-9], thus limiting the available number of healthy cells for use in developing these constructs, and immortalization of cultured HCEC to increase the number of cells available for human transplant is problematic. If successful, the new approach being tested in this study will permit repair of corneal endothelium and restoration of clear vision without the need for donor corneal tissue. The GOAL of these studies is to develop a new approach to the repair of injured corneal endothelium by testing whether human umbilical cord blood mesenchymal stem cells (UCB MSC) can integrate into the injured endothelium and differentiate to form functional HCEC-like cells.

This project was conducted in collaboration with Biagio Saitta, Ph.D., University of Medicine and Dentistry of New Jersey, who has considerable experience in the isolation and characterization of mesenchymal stem/stromal cells from human umbilical cord blood[10]. We received 2 types of UCB MSCs from Dr. Saitta, designated Type 1 and MSC34b. These 2 types of UCB MSCs exhibit the morphological and genetic characteristics expected for MSCs[11,12]. That is, they both adhere to tissue culture plastic and have a fibroblast-like morphology. They also express the MSC-specific markers, CD73, CD90, and CD105, and do not express the hematopoeitic markers CD11b, CD34, or CD45. Comparison of an isogenic population of UCB MSCs indicated the presence of 2 populations with somewhat different growth kinetics, immunophenotype, and differentiation potential. UCB Type 1 MSCs appear as highly elongated fibroblast-like cells that tend to grow in whorls. These cells exhibit faster growth kinetics, higher population doublings, and have a greater potential to differentiate along the adipogenic lineage. UCB Type 2 MSCs (designated MSC34b in these studies) retain a fibroblast-

like morphology, but are less elongated and tend to cluster in groups, although they do not form a confluent monolayer. These cells have slower growth kinetics and have a stronger potential to differentiate along the osteogenic lineage. Over the past year, we concentrated our studies using UCB Type 1 MSCs; however, in the 4th quarter, we initiated studies using UCB Type 2 MSCs (MSC34b) to begin to compare the relative ability of these two MSC types to differentiate to form HCEC-like cells.
These studies used donor human corneas obtained from National Disease Research Interchange (NDRI), Philadelphia, PA. NDRI is an NIH-approved supplier of tissue for basic research. The Schepens Institutional Review Board (IRB) approved the use and handling of this tissue.

BODY:
Research Accomplishments: The description of studies below is a summary of work accomplished and research findings for the entire one-year subproject period.

Prior to conducting the experiments outlined in the Specific Aims, we accomplished the following: 1) Prepared lens epithelial cell-conditioned medium; 2) Expanded cultures of GFP-labeled UCB Type 1 and MSC34b cells; and 3) Labeled additional cells with Q-Tracker so that they could be followed by fluorescence microscopy. Two Specific Aims were proposed for this project.

Specific Aim #1: Test the ability of UCB MSCs to attach to Descemet's membrane and integrate into areas of endothelial injury. Two ex vivo corneal wound models were employed using donor corneas with normal endothelial cell densities (ECD: $\geq$ 2000 cells/mm^2). In one wound model, the endothelium was gently scraped in an X-pattern, leaving Descemet's membrane intact, but denuded of endothelial cells. A second wound model involved making a crush wound with a blunt forceps in order to damage endothelial cells, but not denude Descemet's membrane of cells. A third ex vivo model used unwounded donor corneas with low ECD ($\leq$ 1500 cell/mm^2). The majority of studies were conducted using UCB Type 1 MSCs, although we began studies to compare and contrast the responses of MSC34b. Corneas with seeded MSCs were incubated in basal medium (DMEM with low glucose, 20% fetal bovine serum, and pen/strep) in the presence and absence of the same medium conditioned by incubation with human lens epithelial cells prepared at a 1:1 dilution. The end-point for most experiments was Day 14. We observed the following:

- Neither UCB Type 1 MSCs nor MSC34b cells attach with strong affinity to undamaged, healthy HCEC.

- Neither UCB Type 1 MSCs nor MSC34b cells attach to areas of Descemet's membrane denuded of HCEC.

- Both UCB Type 1 MSCs and MSC34b cells were able to detect damaged HCEC and to attach to these areas of damage.

- There was no observable difference in the ability of either type of MSC to attach to damaged endothelial cells based on the nature of the culture medium.

- Under the experimental conditions used, neither UCB Type 1 MSCs nor MSC34b cells became fully integrated into areas of endothelial injury. That is, they did not help re-form a monolayer in the damaged areas. Neither type of MSC showed significant staining for Ki67 (a marker of proliferating cells), indicating that cells did not divide to fill the space occupied by damaged HCEC, resulting in an insufficient number of MSCs to fully cover the wounded area.

Specific Aim #2: Test the ability of adherent UCB MSCs to differentiate to form HCEC-like cells.

The majority of the studies under this specific aim were conducted using UCB Type 1 MSCs. Cells were applied to donor human corneas using the 2 ex vivo wound models and to unwounded donor human corneas with low ECD, as described above. MSC34b were applied to a crush wound of the endothelium. In both cases, corneas were incubated in basal medium and lens epithelial cell-conditioned medium, as described above. We observed the following:

- In the presence of lens epithelial cell-conditioned medium, there was a change in the shape of individual UCB Type 1 MSCs from their normally elongated form to a more spread, flat, HCEC-like shape.

- These spread cells also appeared to up-regulate their expression of ZO-1, a tight junction-associated protein, as shown by an increase in fluorescence intensity. We did not find evidence that these cells actually formed tight junctions either between themselves or with HCEC, since ZO-1 was observed in the MSCs as diffuse cytoplasmic staining, rather than as an intense stain located at the cell periphery.

- In the presence of lens epithelial cell-conditioned medium, MSC34b cells attached to damaged endothelium in clusters, but did not significantly alter their shape. Cells appeared to up-regulate the expression of ZO-1 in a manner similar to that of UCB Type 1 MSCs.

We also conducted an experiment to test whether we could immunostain for the mesenchymal cell marker, CD90 (Thy-1), as an alternative to fluorescently labeling the MSCs. CD90 was previously shown by our consultant, Dr. Biagio Saitta, to be expressed by UCB MSCs; however, there was no available information regarding expression of CD90 in HCEC. Unfortunately, immuocytochemical localization studies and Western blot analyses found that CD90 is also expressed by HCEC, making this marker useless for immunocytochemically distinguishing the two cell types. What it DOES indicate is the relatively close relationship between UCB MSCs and HCECs, providing additional

evidence that we should be able to find microenvironmental conditions that will facilitate the differentiation of these MSCs to HCEC-like cells.

Relationship of the most recent findings with that of previously reported findings: There are no new published articles regarding the differentiation of mesenchymal stem cells to form HCEC-like cells other than the article cited in the 1st Quarterly Report.

Problems Associated with Accomplishing the Proposed Tasks: The problems discussed under #2 in this section of the 2nd quarterly report were addressed during the 3rd quarter.

KEY RESEARCH ACCOMPLISHMENTS:

- Determined that wound size and relative MSC seeding density are important for more complete coverage of damaged corneal endothelium by the MSCs. This has led to a modification of our original mechanical wounding protocol.

- Observed attachment of Type 1 UCB MSCs and Type 2 UCB MSC34b to areas of the wounded endothelium using two ex vivo corneal endothelial wound models. These observations show consistency and specificity in attachment of these MSCs to injured endothelium rather than to uninjured endothelium or to Descemet's membrane.

- Observed attachment of Type 1 UCB MSCs in unwounded endothelium from corneas with low ECD, indicating that the MSCs can detect and "home" to "stressed" cells that have not been mechanically wounded.

- Observed that lens epithelial cell-conditioned medium can alter the morphology of Type 1 UCB MSCs from a thin, elongated shape to a flat spread shape. This shape is closer to the morphology of corneal endothelial cells. In these flatter cells, we also observed increased staining for ZO-1, which was diffusely distributed within the cytoplasm. This finding suggests that ZO-1 synthesis is up-regulated in these cells, but that normal tight junctions have not yet formed. Together, results provide suggestive evidence that Type 1 UCB MSCs can be induced to differentiate toward a corneal endothelial cell-like phenotype, particularly in the presence of lens epithelial cell-conditioned medium.

- Observed that lens epithelial cell-conditioned medium also increases the expression of ZO-1 in Type 2 MSC34b cells. As with Type 1 MSCs, the cellular distribution is diffuse in the cytoplasm.

REPORTABLE OUTCOMES:

- No publications have resulted from these studies, since they were designed to simply explore a new tissue engineering method.

- Information obtained from studies conducted under this subproject has been applied to studies of MSC differentiation currently being conducted under an NIH-funded R21 grant.

CONCLUSIONS:

- Type 1 UCB MSCs and Type 2 MSC34b cells are able to specifically recognize and attach to injured corneal endothelial cells.

- Lens epithelial cell-conditioned medium contains one or more factors that appear to alter both Type 1 UCB MSCs and Type 2 MSC34b cells to a more HCEC-like phenotype.

- Full differentiation of these MSCs to an HCEC-like phenotype must take longer than 14 days under the ex vivo conditions used for these experiments.

- Type 1 UCB MSCs and Type 2 MSC34b cells may be useful for healing corneal endothelial wounds.

- Further study of appropriate methods to differentiate human umbilical cord blood mesenchymal stem cells is justified by the results obtained.

REFERENCES:

1. Terry MA, Ousley PJ. Endothelial replacement without surface corneal incisions or sutures: topography of the deep lamellar endothelial keratoplasty procedure. Cornea. 2001;20:14-18.

2. Price FW Jr., Price MO. Descemet's stripping with endothelial keratoplasty in 200 eyes: Early challenges and techniques to enhance donor adherence. J Cataract Refract Surg. 2006;32:411-418.

3. Melles GR, Ong TS, Ververs B, van der Wees J. Descemet membrane endothelial keratoplasty. Cornea. 2006;25:987-990.

4. Griffith M, Osborne R, Munger R., et al. Functional human corneal equivalents constructed from cell lines. Science. 1999;286:2169-2172.

5. Lai JY, Chen KH, Hsiue GH. Tissue-engineered human corneal endothelial cell sheet transplantation in a rabbit model using functional biomaterials. Transplantation. 2007;84:1222-1232.

6. Koizumi N, Sakamoto Y, Okumura N, et al. Cultivated corneal endothelial cell sheet transplantation in a primate model. Invest Ophthalmol Vis Sci. 2007;48:4519-4526.

7. Senoo T, Joyce NC. Cell cycle kinetics in corneal endothelium from old and young donors. Invest Ophthalmol Vis Sci. 2000;41:660-666.

8. Chen K-H, Azar D, Joyce NC. Transplantation of adult human corneal endothelium *ex vivo*. Cornea. 2001;20:731-737.

9. Zhu CC, Joyce NC. Proliferative response of corneal endothelial cells from young and older donors. Invest Ophthalmol Vis Sci. 2004;45:1743-1751.

10. Markov V, Kusumi K, Tadesse M, et al. Identification of cord blood-derived mesenchymal stem/stromal cell populations with distinct growth kinetics, differentiation potentials, and gene expression profiles. Stem Cells Dev. 2007;16:53-73.

11. Horwitz EM, LeBlanc K, Dominici M, et al. Clarification of the nomenclature for MSC: The International Society for Cellular Therapy position statement. Cytotherapy. 2005;7:393-395.

12. Dominici M, LeBlank K, Mueller I, et al. Minimal criteria for defining multipotent mesenchymal stromal cells. The International Society for Cellular Therapy position statement. Cytotherapy. 2006;8:315-317.

Task 5
Joan Stein-Streilein, Ph.D.
Title: Loss of Immune Privilege and Retinal Laser Burn
Determine retinal laser burn (RLB)-induced mechanisms that lead to novel immune inflammatory responses, and functional changes in the retina that abrogate ocular immune privilege in the contralateral as well as the burned eye**.**

INTRODUCTION:
Immune privileged is a term that describes tissue sites that promote prolonged or indefinite acceptance of foreign tissues. Immune privilege, in part, is mediated by the development of immune responses that lack inflammatory aspects. Thus, when antigens are inoculated into the eye, an immune response is generated that lacks T effector cells and B cells capable of making complement fixing antibodies. However, B cells that make non-complement fixing antibodies are present and antigen specific T regulatory cells develop which promote tolerance both locally and systemically. It is not surprising that the eye is an immune privileged site, since unwanted inflammation in the eye would interfere with the path of light that focuses images on the retina. However, if immune privilege is compromised, inflammation can occur in the eye and persistent and chronic immune inflammatory response may lead to visual problems and even blindness. Thus, understanding the conditions that disturb the balance between the immune regulation and inflammation in the eye may lead to novel therapies that restore immune privilege and improve the clinical situation.

In an attempt to understand the mechanisms that might lead to loss of immune privilege and the development of inflammation in the eye, a retinal laser burn (RLB) model is used

to study how inflammation in the back of the eye might interfere with immune privilege throughout the eye. We postulate that RLB in part changes the immunosuppressive environment of the eye and subsequently the tolerogenic ability of indigenous cells.

BODY:

Objective 1: To determine the cause of RLB induced loss of immune privilege in the burned eye.

Findings:

Since RLB affected the immune privilege of both eyes, burned and non-burned, we postulated that a neuronal signal might induce inflammatory signals in both eyes. Substance P is produced by neurons and non-neuronal cells like lymphocytes and is reported to induce three of the proinflammatory cytokines that could be in the burned eye (IL-6, IL-1β and TNF-α). In ACAID, Ferguson and others (1995) found that Substance P is elevated in mice that were dark-reared. Subsequently, dark reared mice lose their ability to induce ACAID. Moreover, blocking Substance P binding reversed the loss of ACAID, thus showing that Substance P was the antagonist of ACAID. Thus we postulated that Substance P might be interfering with our ability to induce ACAID post RLB. To assess the role of Substance P in abrogation of ACAID post-RLB, we induced ACAID in WT or Substance P Knockout (KO) mice. As expected ACAID was not induced in C57BL/6J mice that received RLB treatment followed a.c. inoculation of OVA into the burned or non-burned eye.(Figure 1A). Substance P KO mice that received RLB prior to antigen (a.c.) into the burned or non-burned eye developed ACAID (Figure 1B). Thus, Substance P maybe an important factor in the loss of ACAID in mice post-RLB treatment.

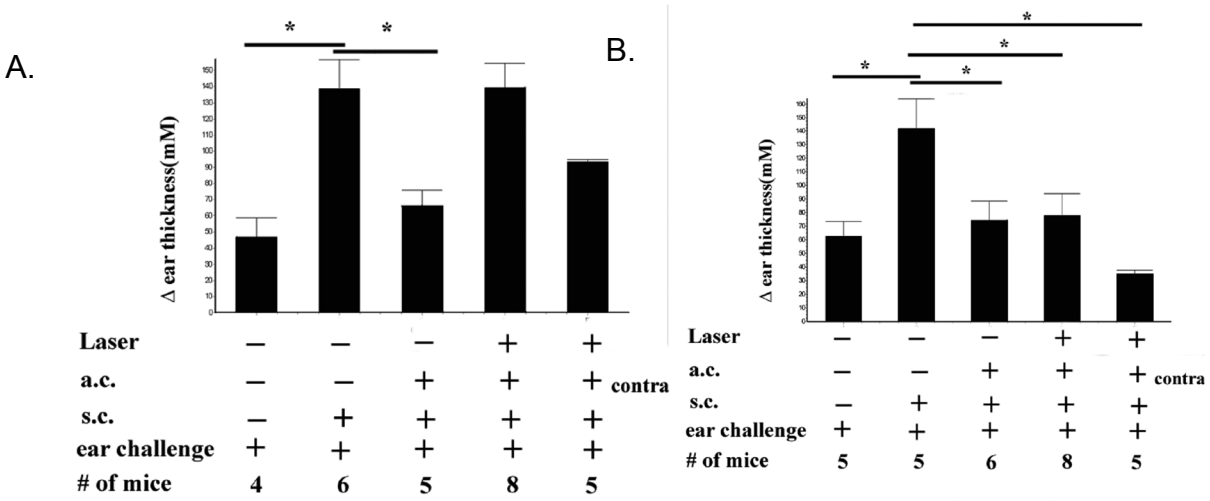

Figure 1. Induction of ACAID after RLB treatment in WT or Substance P KO mice. Analyses of Delayed Hypersensitivity (DH) response in the ear is shown in C57BL/6J (A) or Substance P KO (B) mice. Change of ear thickness is indicated on the ordinate. Treatment of the mice is listed under each bar along the abscissa. Lane 1: negative control, Lane 2: positive control (DH response) , Lane 3: ACAID response; Lane 4: RLB treatment to the right eye and

induction of ACAID in the same eye. * indicates significance P< 0.05 using Bonferroni's Multiple Comparisons Test.

Objective 2: To determine if RLB damage to the retinal pigmented epithelium (RPE) leads to the loss of ACAID in the contralateral eye.

Findings:
Previous studies show that immune privilege (ACAID) is lost in the contralateral eye of mice 1-14 day's post-RLB treatment (Qiao et al., 2009). We have also shown that the ipsilateral RPE (Retinal Pigmented Epithelium) eyecup from mice that received RLB treatment lose their ability to convert T cells into T regulatory cells ($CD8^+$ $FoxP3^+$). Therefore, we wanted to assess the ability of the RPE eyecup of the contralateral eye of mice that received RLB to modulate T cells into T regulatory cells. In brief, eyes were removed from C57BL/6 mice that received RLB treatment to the right eye 24 hours prior to enucleation. RPE eyecups were prepared by dissecting the eye along the ora serreta, the anterior portion and neural retina were discarded. Primed OT1 $CD44^+$ T cells were incubated with RPE eyecups from naïve; the ipsilateral or contralateral eye of RLB treated mice for 48 hours. T cells were collected, stained with CD8 and FoxP3 antibodies, and subjected to flow analysis. As expected, T cells incubated with the RPE eyecup from the ipsilateral did lose the ability to convert T cells into $CD8^+FoxP3^+$ T regulatory cells (Figure 2) (naïve, 1.355% vs. ipsilateral, .77%). However, RPE eyecups prepared from the contralateral eye post-RLB did not lose the ability to convert activated T cells into $CD8^+FoxP3^+$ T regulatory cells (naïve, 1.355% vs. contralateral, 1.745%). These data suggest that the suppressive function of the RPE in the contralateral eye post-RLB is intact, therefore the immune privilege mechanisms controlling RPE suppressor function vs ACAID are different, since ACAID is lost in the contralateral eye of RLB mice.

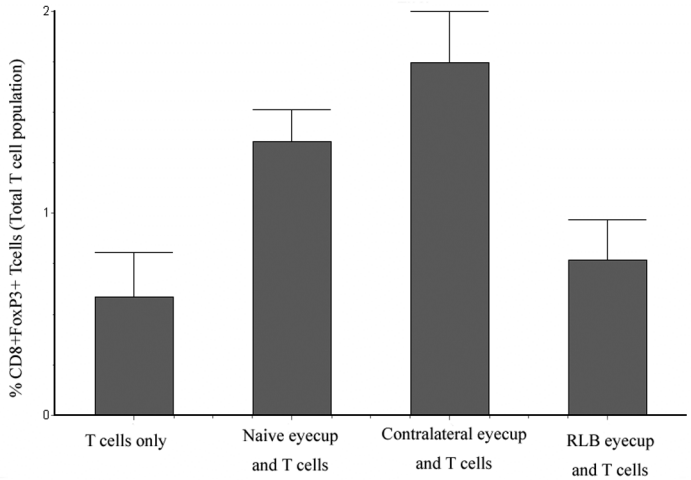

Figure 2. Flow cytometry analysis of T cells stained with CD8 and FoxP3 antibodies. Quantification of $CD8^+FoxP3^+$ T cells from the total T cell population. $CD44^+$ T cells from primed OT1 mice were incubated for 48hrs with naïve RPE eyecups (Lane 2) or contralateral

(Lane 3) or ipsilateral (Lane 4) RPE eyecup of RLB treated mice. T cells were stained with CD8 and FoxP3 antibodies and subjected to flow analysis. Percent of $CD8^{+}FoxP3^{+}$ cells of the total T cell population (ordinate). Treatment of eyecups below the abscissa. N=4 mice.

Our previous studies showed that ACAID is lost in the burned eye as early as 6 hours and as late as 56 days post RLB. Additionally, ACAID is lost in the contralateral (non-burned) eye 21 days post-RLB. Thus, we assayed if the loss of ACAID in the burned and non-burned eye is long lasting. C57BL/6 mice received RLB to the right eye. ACAID was induced in non-treated or treated mice 1, 68 or 77 days post RLB. As expected, immune privilege was present in ACAID mice (Figure 3, lane 3). However, mice that received RLB treatment and a.c. injection of OVA injection into the burned eye 77 days post-RLB (Figure 3, Lane 6) had no significant difference in ear swelling compared to immunized mice. Surprisingly, mice that received RLB treatment followed by a.c. injection of OVA into the non-burned eye 68 days post RLB also lost immune privilege. This data suggest that loss of immune privilege is persistent in both the burned and non-burned (contralateral) eye after RLB.

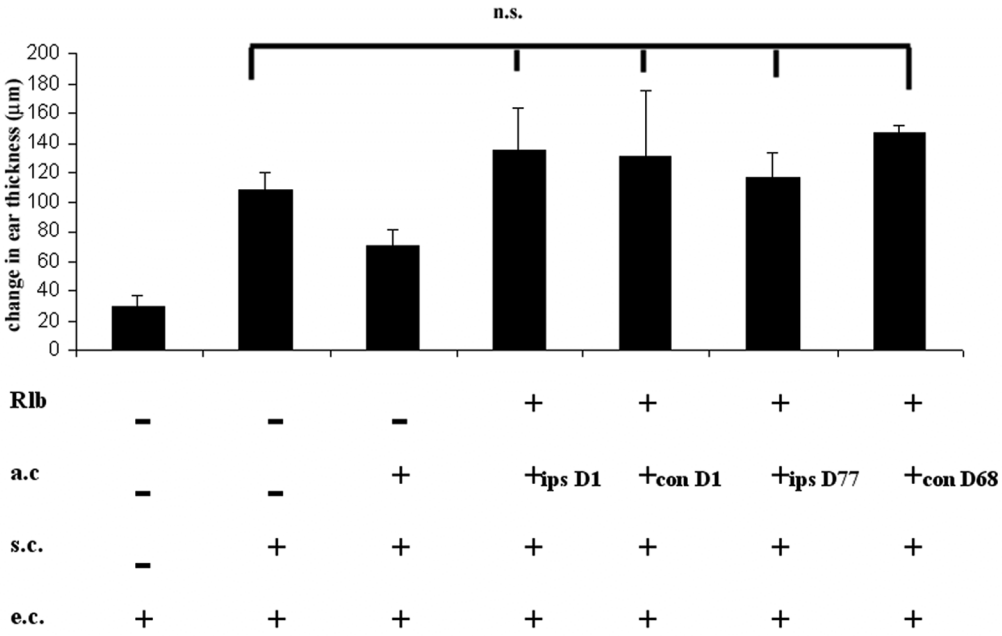

Figure 3: Induction of ACAID in the ipsilateral or contralateral eye 68 or 77 days post-RLB treatment. Lane 1: negative control, Lane 2: positive control , Lane 3: ACAID treatment, Lane 4: RLB treatment to the right eye followed by an a.c. injection to the right eye 1 day post-RLB, Lane 5 RLB treatment to the right eye followed by an a.c. injection to the left eye 1 day post-RLB. Lane 6: RLB treatment to the right eye followed by an a.c. injection to the right eye 77 days post-RLB, Lane 7 RLB treatment to the right eye followed by an a.c. injection to the left eye 68 days post-RLB. n.s. indicates no significant difference. Statistics ANOVA, Bonferroni Multiple Comparisons Test (3-5 mice per treatment).

REPORTABLE OUTCOMES:

A manuscript entitled "Retinal laser burn disrupts immune privilege in the eye" has been published in the American Journal of Pathology 2009 Feb;174(2):414-22..

Abstract:
Lucas KG and Stein-Streilein J. Role of Neuropeptides in the Loss of Immune Privilege After RLB. Association for Research in Vision and Ophthalmology 2010, Fort Lauderdale, FL, 2010.

CONCLUSION:
1. RLB abrogates immune privilege in part by breaking the blood ocular barrier, allowing an influx of inflammatory cells. Compared to C57BL/6J, Substance P KO mice appear not to lose the ability to induce ACAID after RLB treatment. Thus, Substance P maybe critical for loss of the ACAID in mice post RLB treatment .

2. The suppressive function of the RPE in the contralateral eye post-RLB is intact, therefore the immune privilege mechanisms controlling RPE suppressor function vs ACAID are different, since ACAID is lost in the contralateral eye of RLB mice. Further studies are needed to determine the mechanism. This model may be used as a model of sympathetic ophthalmia in which trauma to one eye leads to blindness in the contralateral unharmed eye.

3. Immune privilege is lost in both the burned and non-burned eye 77 and 68 days respectively, after RLB treatment. Thus, lose of immune privilege is a long lasting event in RLB treated mice.

REFERENCES:
H. Qiao, K. Lucas, J. Stein-Streilein, *Am J Pathol* **174**, 414 (Feb 2009).

Task 6
Dong Feng Chen, M.D., Ph.D.
Title: Potential Therapy for Retinal Laser Injury by Activating the Dormant Neuroregenerative Potential of Adult Muller Glia with Sonic Hedgehog Signaling

INTRODUCTION:
The objective of the present research is to study the molecular mechanisms that regulate retinal stem cell potency with a goal of developing stem cell regenerative therapy for retinal injury. In adult mammals, damage to the retina as a result of disease or injury can lead to permanent loss of vision because their neurons regenerate poorly. The pigmented cells in ciliary body (ciliary epithelium, CE) are considered a source of retinal stem cells, which exhibit the multi-potency of differentiation into all types of retinal neurons in culture. However, a recent report suggests that these CE-derived cells exhibit primarily pigmented ciliary epithelial cell properties with low neurogenic potential. This study has raised the important question whether the neurogenic potential of CE-derived cells can revived for repairing the damaged retina after disease or injury. To date, little is known about the signaling events that regulate the neurogenic potential of CE-derived cells.

Molecular signals that are reported to be involved in the regulation of neural progenitor cell potency include Sonic Hedgehog, wnt, and ephrins. During development, these

molecules play crucial roles that act a positive or negative growth signals for neural stem cells. Ephrins and Eph receptors are pivotal regulators of pattern formation, cell migration, axonal guidance, and synaptogenesis during CNS development. Recent studies indicate that ephrin-As, functioning through their receptor EphA7, negatively regulate neural stem cell survival and proliferation in the developing telencephalon and adult supra ventricular zone (SVZ). Reports from our lab further indicate that their expression in the adult CNS suppresses neurogenic potential of stem cells in the non-conventional neurogenic CNS regions. To identify the role of ephrinAs in retinal stem cell potency, we studied the proliferation and differentiation of CE-derived cells in ephrinA3 knockout mice.

BODY:

Expression of ephrin-A3 in the retina and ciliary body of adult mice

To examine the role of ephrinA3 in retinal stem cells, we studied the temporal and spatial expression profile of ephrinA3 in the mouse retina (Fig. 1). Analysis of Western blot indicates that the expression of ephrinA3 was undetectable in the embryonic retina where there was active neurogenesis (Fig. 1E). EphrinA3 appeared on P10 retina, when retinal neurogenesis ceases, and reached the peak in the adult (Fig 1E). This pattern of expression is consistent with the reduction of retinal stem cell proliferation during retinal mature. Results of immunostaining further proved ephrinA3 expression in the mature retina (Fig. 1A, 1C) and the ciliary body (Fig 1B, 1D), suggesting its involvement in the regulation of the proliferation and neurogenic potential of retinal stem cells and CE-derived cells.

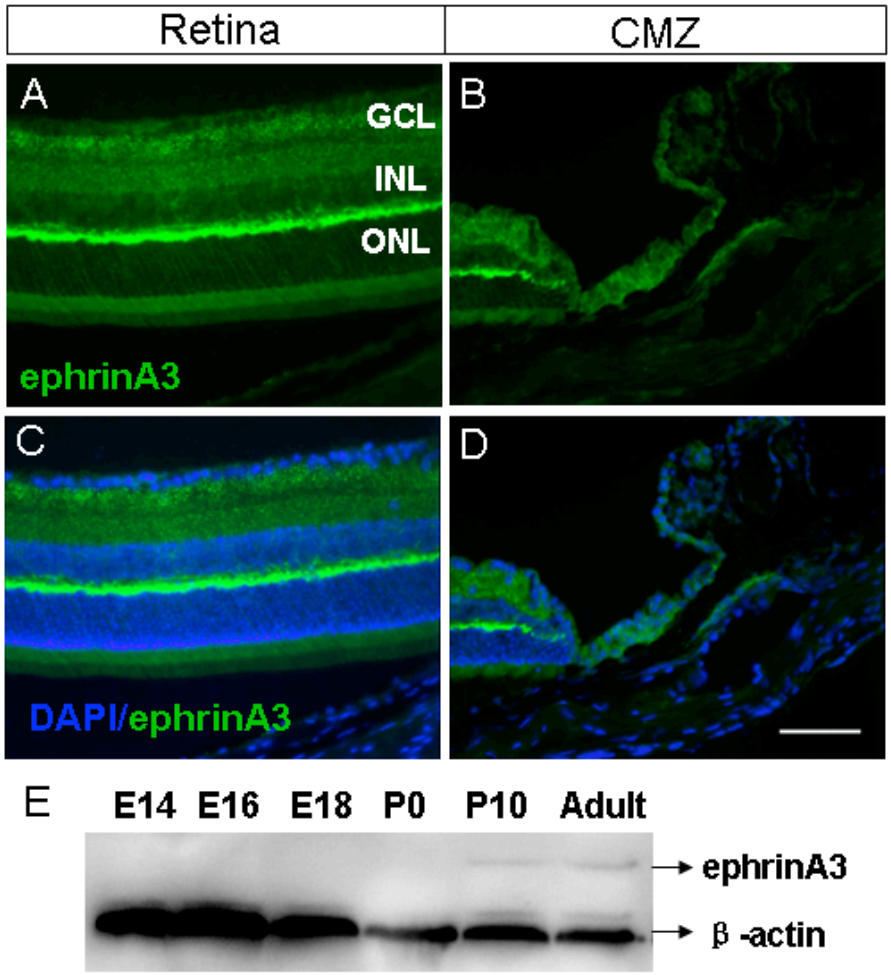

Fig. 1. EphrinA3 expression profile in the mouse eye. A-D, Epifluorescence photomicrographs of ephrinA3 immonulabeling (green) in the retina (A,C) and ciliary body (B,D). The retinal sections were counterstained with a nuclear marker DAPI (blue) to reveal the laminar structure (C,D). Expression of ephrinA3 was detected strongly in the retina (A,C) and ciliary body (B,D) of adult mice. Scale bar: 100μm. E, Western blot analysis of ephrinA3 expression in the retinas of mice at different ages. Note the expression of ephrinA3 started to appear in the mouse retina at around P10. In adult mouse eye, the ephrinA3 was detected strongly on retina (C, E) and weekly on ciliary marginal zone (CMZ) (D, F) by immunostaining. Bar: 100μm.

Increased proliferation of retinal progenitors in ephrinA3 deficient mice

To determine whether ephrinA3 plays a negative role on CE-derived retinal progenitors, adult wild-type and ephrinA3-/- mice were injected with BrdU (50 mg/Kg, i.p.). Mice were sacrificed 7 days after BrdU pulse labeling. BrdU+ cells were noted in the ciliary body and peripheral retina of adult ephrinA3-/- mouse, while very few was seen in that of wild-type mice. These BrdU+ cells were co-stained by antibodies recognizing retinal progenitor cell markers—Chx10 and nestin (not shown)—suggesting that the proliferating cells were retinal progenitors. There was a significant increase in number of BrdU-positive cells in the ciliary margin of adult ephrinA3-/- mice as compared to that in

wildtype mice.

To further test that absence of ephrinA3 promotes the proliferation of retinal progenitor cells at the ciliary margin, we investigated neurosphere formation in CE-derived cell cultures. Similar number of CE-derived cells of adult wild-type and ephrinA3-/- mice were seeded in 48-well plates and cultured in EGF and FGF containing medium. After 14 days of incubation, we noted a significant increase in the number of primary neurospheres in cultures derived from ephrinA3-/- mice as compared to that of wild-type mice (Fig. 2). Primary neurospheres derived from wild-type and ephrinA3-/- mice were dissociated and then seeded at a single cell density in 48-well plates. After 14 days of culturing, we found that the numbers of secondary neurospheres derived from ephrinA3-/- mice were also significantly higher than that of wild-type neurospheres (Fig. 2F). In agreement with this finding, we found that the ratio of BrdU incorporation in cells dissociated from neurospheres of ephrinA3-/- mice was significantly higher than that dissociated from wild-type mice (Fig. 2G). In contrast, addition of antibody-clustered ephrinA3 proteins into retinal progenitor cell cultures diminished BrdU incorporation as compared to control Fc-treated group (Fig. 2H). Together, these results clearly indicate that ephrinA3 functions as a negative regulator for the proliferation of retinal progenitor cells derived from the ciliary margin.

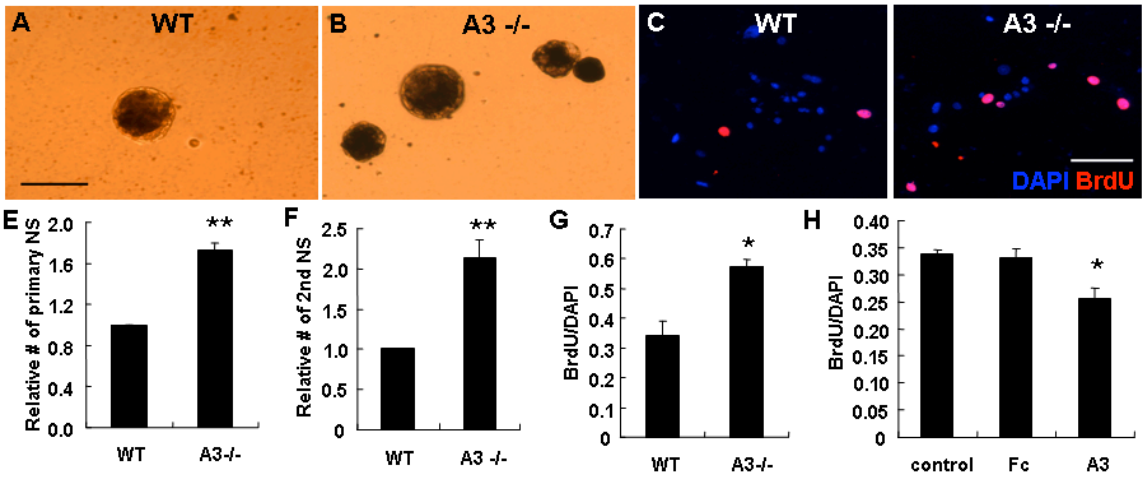

Fig. 2. Increased proliferation of retinal progenitor cells derived from ephrinA3-/- mice. **A,B,** Formation of primary neurospheres (NS) in CE-derived cell cultures of adult wild-type (WT) and ephrinA3-/- (A3-/-) mice. Scale bar: 100 µm. **C,D,** BudU incorporation (red) into dissociated cell cultures that isolated from CE-derived NS of WT and A3-/- mice. Cell cultures were countered stained with a nuclear marker, DAPI (blue). Scale bar: 50 µm. **E-H,** Quantification of primary (E) and secondary (F) NS numbers in CE-derived cells of A3-/- mice in relative to that of cultures prepared from WT mice and quantification of BrdU incorporation (G,H) in dissociated NS cells derived from WT or A3-/- mice (G) or in dissociated NS cells of WT mice that were treated with control Fc or antibody clustered A3 (A3). Note the increased number of primary and secondary NS formed in cultures prepared from ephrinA3-/- mice as compared to that of WT mice (*P<0.05; **P<0.01; student's t test; n=3/group)**Absence of ephrinA3 increased progenitor cell potency of CE-derived cells**

To determine whether absence of ephrinA3 alters the progenitor cell potency of CE-derived cells, we examined the levels of expression of progenitor cell markers in neurospheres using quantitative PCR. GAPDH and β-actin were used as internal control. We noted that the levels of retinal progenitor cell markers, such as Chx10, Sox2, wnt3a and wnt7a, were significantly upregulated in neurosphere-derived cells of ephrinA3-/- mice (Fig. 3), implicating an increased progenitor cell potency. Moreover, we found that CE-derived retinal progenitors of ephrinA3-/- mice exhibited higher levels of retinal photoreceptor precursor cell markers, that included Crx, Nrl, Ngn2 and Nr2e3 than that from wild-type mice, indicating an increased cell fate for retinal and photoreceptor cell differentiation in the absence of ephrinA3 (Fig. 3C). In contrast, expression of retinal pigment epithelial cell marker, such as Mift, was significally down regulated in neurospheres derived from ephrinA3-/- mice as compared to that of wild-type mice (Fig. 3B). The data support that ephrinA3 negatively regulates retinal progenitor cell potency and that absence of eprinA3 resulted in a switch of cell fate from pigmented progenitor cells to retinal progenitor cells.

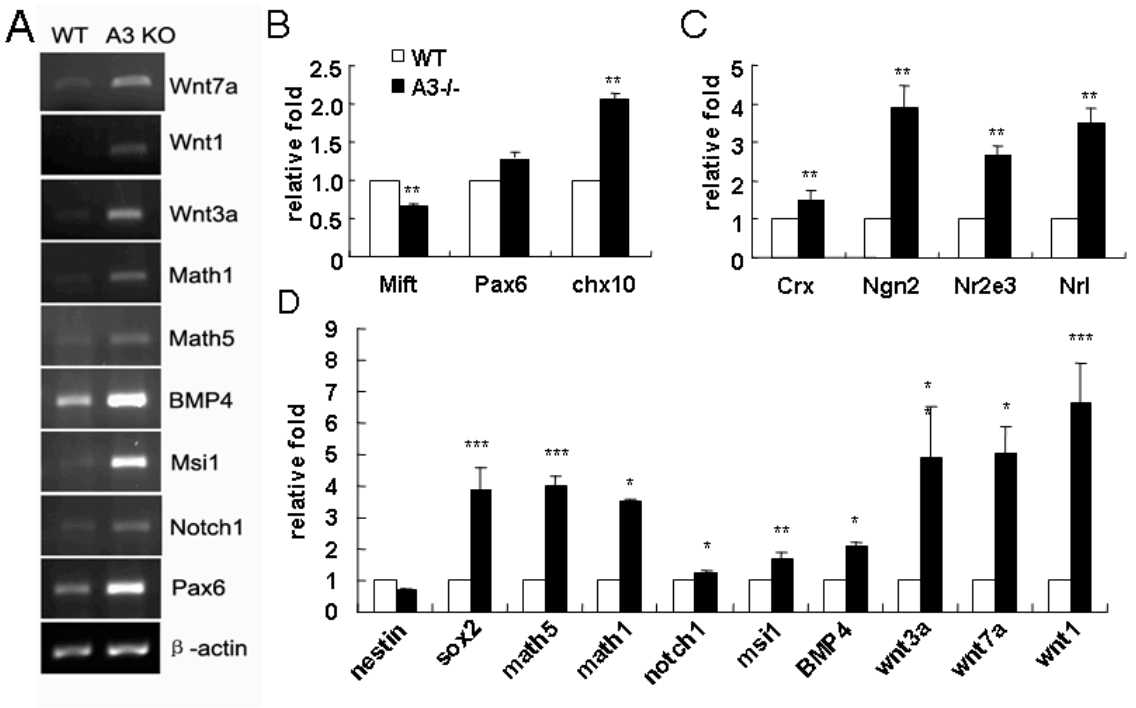

Fig. 3. CE-derived cells upregulates retinal stem cell markers in the absence of ephrinA3. A, Representative RT-PCR (A) and quantification (B-D) of mRNA levels of various genes in neurospheres isolated from wild-type (WT) and ephrinA3-/- (A3 KO) mice. (**P*<0.05; ***P*<0.01; ****P*<0.001; Student's t test and Mann-Whitney Rank Sum Test)

EphrinA3 suppresses wnt signaling to regulate retinal progenitor cell proliferation

Next, we investigated the signaling events through which ephrinA3 suppresses retinal progenitor cells fate. Since deletion of ephrin A3 significantly increased the level of the

neurogenic signals and Wnt family proteins, we asked whether ephrinA3 suppresses the Wnt pathways to regulate the cell fate switch of CE-derived progenitors. We found that application of Wnt3a to dissociated CE-derived retinal progenitor cell cultures significantly increased the level of beta-catenin and BrdU incorporation. The BrdU incorporation ratio in Wnt3a-treated group was over 2-fold higher than that of the control cultures. Moreover, the expression level of beta-catenin in primary neurospheres derived from ephrinA3-/- mice was also higher than that from wild-type mice, suggesting that absence of ephrinA3 activates the Wnt3a/beta-catenin pathway. Thus, we conclude that ephrinA3 acts through wnt/beta-catenin pathway to supress the proliferation and differentiation of CE-derived retinal progenitor cells.

KEY RESEARCH ACCOMPLISHMENTS:

- Ephrin-A3 presents a negative signal and prohibitory niche in the adult CE local environment to suppress retinal stem cell potency of CE-derived cells.
- Absence of ephrin-A3 greatly enhances endogenous wnt signaling in CE-derived RSCs and results in the increased expression of retinal progenitor cell markers and photoreceptor precursor cell progeny.
- Ephrin-A3 acts through suppressing Wnt/beta-catenin signaling to regulate the proliferation and differentiation of retinal progenitors.
- By manipulating ephrin signaling, CE-derived cells can serve an endogenous source of retinal progenitors for the treatment of photoreceptor damage or degenerative disorders.

REPORTABLE OUTCOMES:

Yuan Fang, Kissaou Tchedre, Jiawei Jiao, and Dong Feng Chen. (2009) EphrinA3 inhibits the proliferation and neuronal potential of retinal stem cells in adult mouse. 2009 *Harvard Stem Cell Institute Annual Retreat.* Abstract.

Fang Y, Tchedre K, Cho K, Sun, X and Chen DF. (2010) EphrinA3 regulates Wnt signaling to control retinal stem cell potency. *manuscript in preparation*

CONCLUSION:

We report that, negative growth signal of CNS neural stem cells, ephrin-A3, presents a strong prohibitory niche in the adult CE local environment and suppresses neural stem cell potency of CE-derived cells. Absence of ephrin-A3 greatly enhanced endogenous wnt signaling in CE-derived RSCs and resulted in the increased expression of retinal progenitor cell markers and photoreceptor progeny. These data suggest that CE-derived RSCs can serve an endogenous source of neural progenitors for the treatment of photoreceptor damage or degenerative disorders by manipulating ephrin signaling pathways.

Task 7

Kameran Lashkari, M.D. (PI)**,** Guochun Chen M.D., Ph.D., Dongfeng Chen M.D., Ph.D., (consultant)

Title: Using Neuronal Progenitor Cells Derived From Persistent Fetal Vasculature to Replace Lost Retinal Ganglion Cells in Traumatic Optic Nerve Injury Associated with Closed Head Trauma

The goal of this proposal is to evaluate whether cells derived from persistent fetal vasculature (PFV) can replace lost retinal ganglion cells that form the optic nerve in a model of optic nerve injury, and whether their integration can be enhanced with the use of the drug alpha-aminoadipate.

Introduction:

Traumatic brain injury (TBI) can have deleterious effects on future functionality of the military personnel. One of the complications of TBI is traumatic optic nerve injury (TONI), in which there is death or loss of the optic nerve neurons due to shock waves transmitted through the skull bones into the apical orbital areas. It is unclear whether TONI is a direct result of cellular damage or secondary to damage to small vessels that feed the optic nerve. The optic nerve often appears normal at presentation and becomes pale and atrophic within 4-8 weeks after injury. This proposal is designed to: (1) examine the capability of adult human progenitor cells (PFV cells) to integrate into the host optic nerve and successfully differentiate into ganglion cells after intravitreal transplantation in both wild-type (non-traumatized) mice and mice with experimental optic nerve crush injury mimicking TONI. (2) Determine whether the drug alpha-aminoadipate (α-AA), a gluatamate agonist, can enhance the integration of these cells by temporarily increasing the permeability of optic nerve head and inner retina to cellular penetration. These results would form the basis for the application PFV cell transplantation into the vitreous of patients with advanced TONI and severe visual loss.

Body:

PVF cells were propagated in tissue culture and infected with adeno-associated virus expressing green fluorescent protein (AAV-GFP). Brdu uptake was assessed in culture and is shown in **Figure 1**. Cells were co-labeled with beta-tubulin III and neurofilament-200 (NF200). Brdu identified two morphologies of PFV cells: (1) small cellular morphology that uptakes Brdu and (2) a more defined "neuronal-like" morphology that does not update Brdu. The latter cells are considered to be neuronally differentiated.

Undifferentiated PFV cells were subjected to qRT-PCR to evaluate the expression of neuronal markers (**Figure 2**). PFV cells express markers that are shared by retinal ganglion cells including thy-1, Brn3a, beta-tubulin III and neurofilament-200. Markers shared by other retina, glial or endothelial elements were not detected.

Intracellular calcium imaging was also performed to determine whether differentiated PFV cells responded to neurotransmitters and calcium agonists. These included glutamate, acetyl choline, GABA, glycine and DOPA. HR is the notation for control vehicle. PFV cells responded to these stimuli by releasing intracellular calcium.

Glutamate showed more rebust response with increased percentage of cells responding to this agent (**Figure 3**).

Transplantation of PFV cells into the vitreous of mice without optic nerve crush injury results in their penetration into the inner portions of the retina (**Figure 4**) into the optic nerve head and intraorbital portion of the optic nerve (**Figure 5**). In Figure 4, PFV cells expressing GFP (green) penetrate the retina up to the inner nuclear layer but fail to differentiate into retinal ganglion cells. In Figure 5, GFP-expressing PFVs fail to form axonal-like structures (please refer to the white square within the figure).

Transplantation of PFVs (GFP, green) into eyes of mice with optic nerve crush injury shows more robust penetration into the inner retinal layers (**Figure 6**). There is an upregulation of GFAP from resident retinal glia. The robust penetration of PFVs may be related to a wound healing response. PFVs penetrate the inner portion of the optic nerve after crush injury. However, they fail to cross the area of crush injury (**Figures 7 & 8**). Figure 8 shows a cross section of the optic nerve with GFP-expressing PFVs within the proximal portion of the optic nerve past the optic nerve head. Additionally, alpha-aminoadipate had no effect on this process.

Key Research Accomplishments:
We have characterized PFV cells in vitro. PFV cells can penetrate the intact retina and optic nerve head into its intraorbital portion after intravitreal injection. PFVs that have migrated into the optic nerve do not readily form axon-like structures. Optic nerve crush injury causes a more robust penetration of PFVs into the inner retina and the optic nerve head. However, PFVs only penetrate the portion of optic nerve proximal to the area of injury, and alpha-aminoadipate has no significant effect on this process. We feel that other adjunct factors may be needed to coax PFVs to cross the area of injury and form functional axons.

Reportable Outcomes:
A manuscript describing the first portions of these experiments has been submitted to Stem Cell Transplantation and is currently under reiew.

Conclusions:
In vitro experiments and data indicate that PFV cells express neuronal markers similar to retinal ganglion cells and respond to neurotransmitters by intracellular calcium release. Transplantation experiments indicate that PFVs have the capacity to penetrate intact retinal and optic nerve tissue, but do not spontaneously form axonal structures in vivo. Transplantation of PFVs after optic nerve crush injury results in more robust penetration into retinal and optic nerve tissue. However, PFVs fail to cross the area of injury. Alpha-aminoadipate does not seem to have an effect on this process.

Figures 1-8:
As follows.

Figure 1. Expression of beta-tubulin III and neurofilament-200 (NF200) in Brdu + and Brdu - cells . Brdu identified two morphologies of PFV cells: (1) small cellular morphology that uptakes Brdu and (2) a more defined "neuronal-like" morphology that does not update Brdu. The latter cells are considered to be neuronally differentiated.

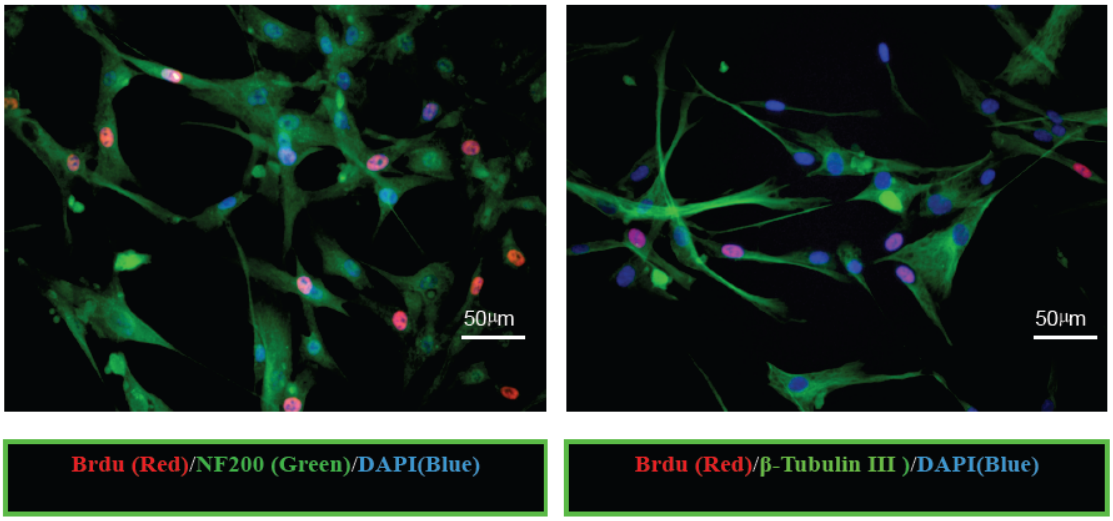

Figure 2. Expression of surface and intracellular markers in undifferentiated PFV cells. RNA samples were collected and subjected to qRT-PCR. + indicates detected of the marker.

Antigenic Profile of undifferentiated PFV cells			
β-Tubulin III	+	Nestin	+
NF200	+	Pax6	+/-
Brn-3a	+	Map5	+
Thy1.1	+	Ki67	+
Synaptophysin	—	Brdu incorporation	+
Recoverin	—	CD34	—
RPE65	—	CD31	—
GFAP	—	CRALBP	—

Figure 3. Intracellular calcium imaging PFV cells in response to various neurotransmitters including Glutamate, Acetyl choline (Acetyl), gama-amino-butyric acide (GABA), glycine, and DOPA. HR is the control vehicle.

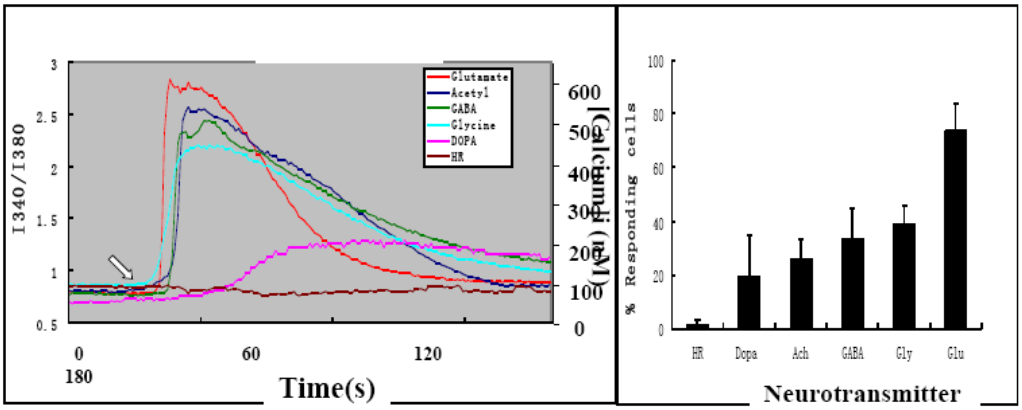

Figure 4. Intravitreal transplantation of PFV cells results in their migration into the inner retinal layers. PFVs express GFP (green).

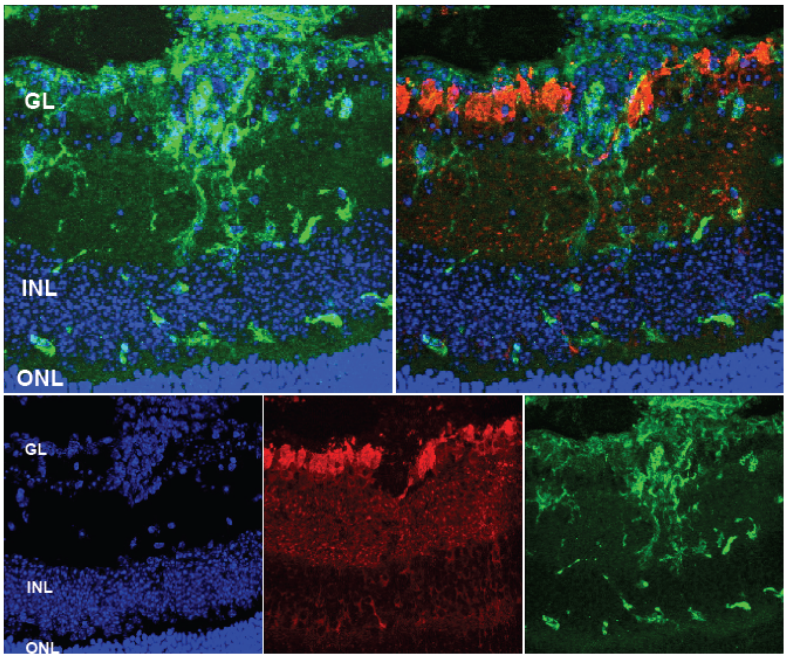

β-III –Tubulin(red)/GFP(green)/DAPI(Blue)

Figure 5. Intravitreal transplantation of PFV also cells results in their migration into the intraorbital portion of the optic nerve. PFVs express GFP (green).

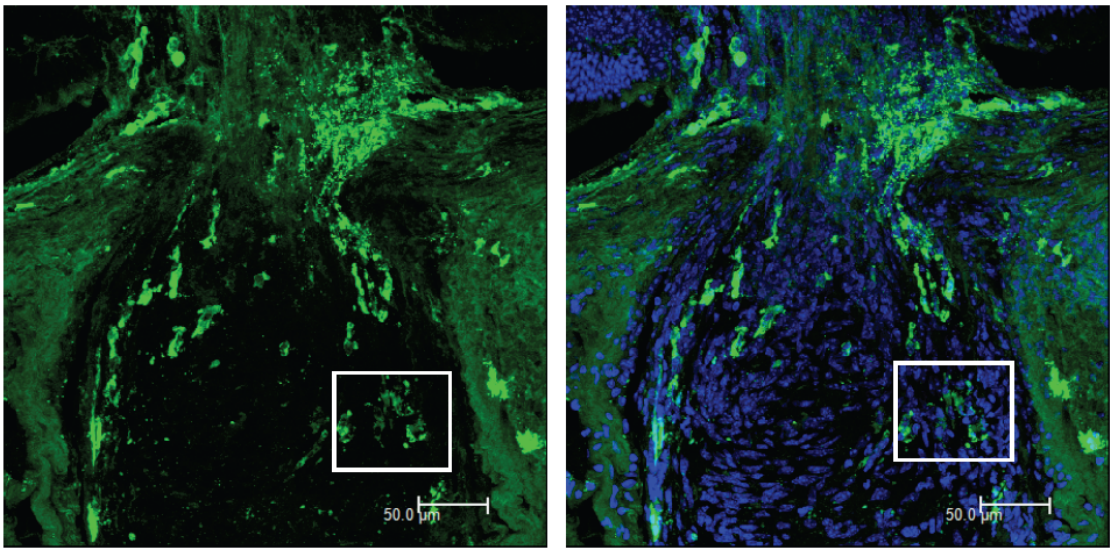

GFP(green)/DAPI(blue)

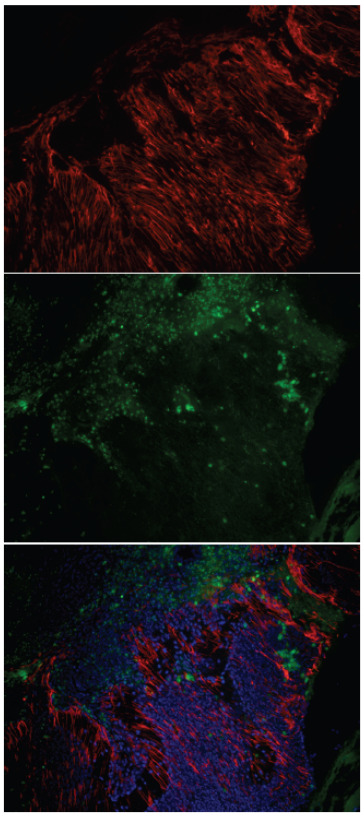

Figure 6. Intravitreal PFVcells penetrate the inner retinal layers in eyes with optic nerve crush injury. Upregulation of GFAP is seen in retinal glia. PFVs express GFP (green).

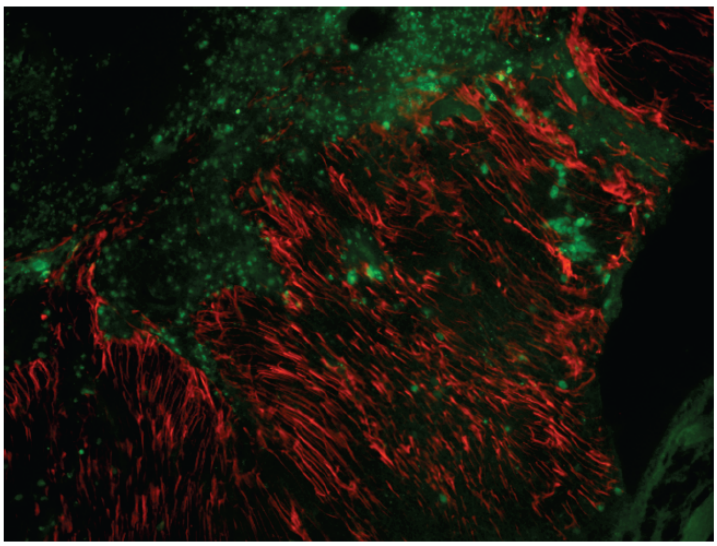

IF staining PFV (green)/GFAP(red)/DAPI(blue) 200x

Figure 7. Intravitreal PFV cells penetrate the inner portions of the optic nerve (arrow) right upto the area of crush injury. Upregulation of GFAP is seen in retinal glia. PFVs express GFP (green).

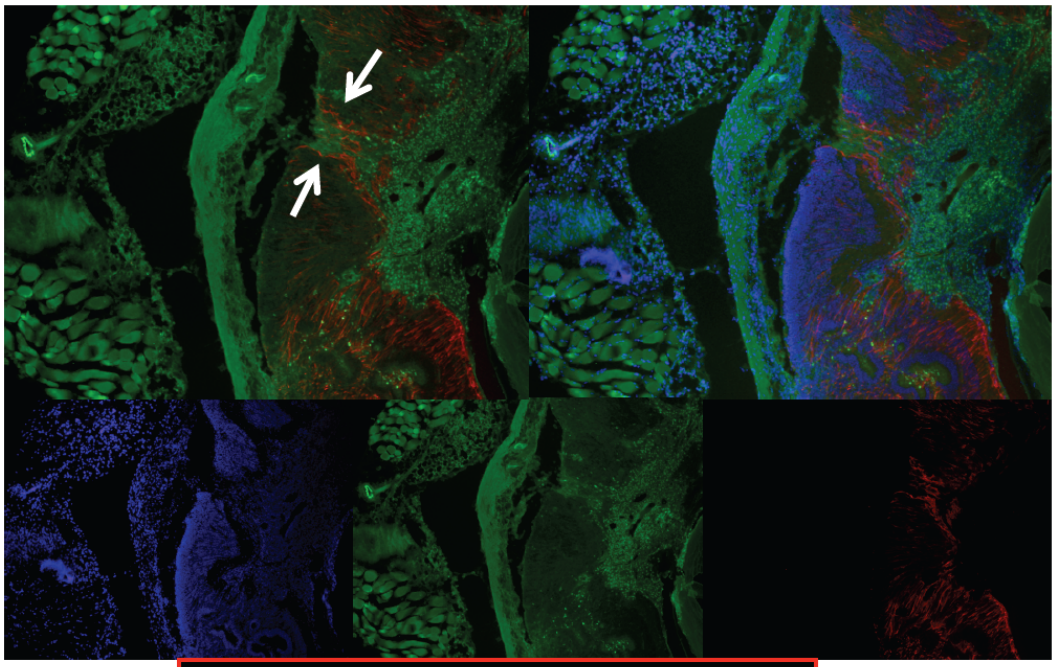

IF staining GFP(green)/GFAP(red)/DAPI(blue) 100x

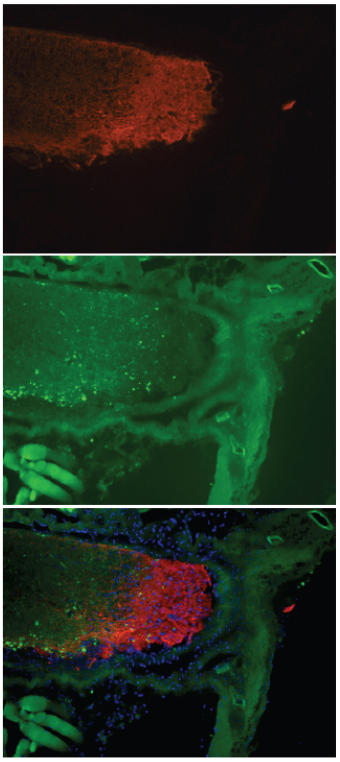

Figure 8. Intravitreal PFV cells penetrate the inner portions of the optic nerve right up to the area of crush injury. Up-regulation of GFAP is seen in retinal glia. PFVs express GFP (green).

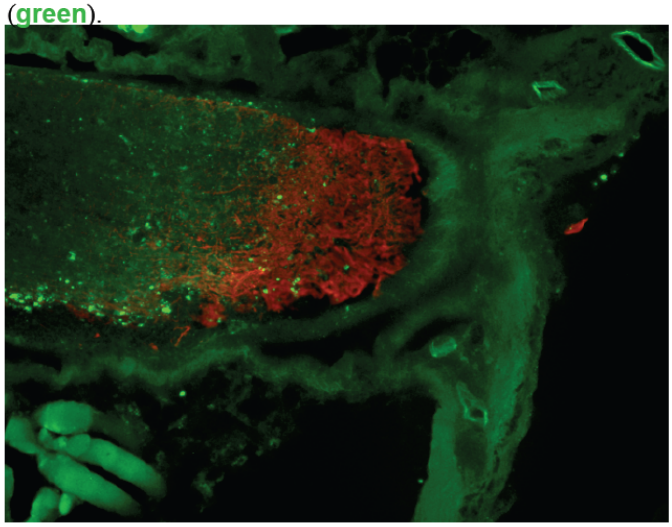

IF staining HLA Class I (green)/GFAP(red)/DAPI(blue) 200x

Task 8
Andrew Taylor, Ph.D.
Title: Applying the mechanisms of ocular immune privilege to diminish microglial cell apoptosis in Traumatic Brain Injury

INTRODUCTION:
While the pathology of traumatic brain injury (TBI) in humans is unclear, in animal models of TBI supportive accessory cells and neurons in the traumatized area of the CNS undergo apoptosis. The loss of functional support cells in the CNS can cause neuropathy beyond the initial site of trauma expanding the region of impaired CNS activity. These support cells are astrocytes and macrophage/microglial cells. Both types of cells support the health of neurons, and provide structural support of the neuronal circuitry. In the immune privileged retina there is a similar role for these support cells. More than just acting as support cells we have found that the healthy retina contains macrophages/microglial cells that mediate immunosuppression. We discovered that intact pigmented retinal epithelial cell layer (RPE) produce the neuropeptide α-MSH that contributes to suppressing inflammatory activity while promoting anti-inflammatory activity by macrophages. When we neutralized α-MSH we found that the macrophages became apoptotic suggesting that α-MSH besides suppressing inflammatory activity while promoting anti-inflammatory activity, it may also promote survival of suppressor macrophages. Recent publications has suggested that a-MSH can prevent the induction of apoptosis in astrocytes, the other type of neuronal support cells, and in hypothalamic neurons, melanocytes, kidney tubular cells, and heart muscle. There is no description of the possible pathways of apoptosis suppressed by α-MSH, except of a hint that α-MSH increases the ratio between Bcl-2 and Bax, two intracellular proteins that regulate anti-apoptotic (Bcl-2) and proapoptotic (Bax) activity within cells Therefore it is our objective to see if this is the case in α-MSH antiapoptotic activity in macrophage/microglial cells. Our long-term objective will be to treat neurologically injured tissues (retina or CNS) with α-MSH or α-MSH analogues. This is to see whether maintaining the health of microglial cells, and possibly other cells, will limit the extent of the lesions in the injured retina or CNS; therefore, minimize the damage to the neurological network needed for maintaining vision and cognitive/motor abilities.

BODY:
The mouse leukemic monocyte macrophage cell line RAW 264.7 cells were cultured in serum-free media, treated with α-MSH for 18 hours, and then assayed for apoptosis. We detected apoptosis using a flow cytometry based assay where the cells were collected, fixed, permeablized, and the fragmented DNA of apoptosis was labeled with FITC-UTP. In the flow cytometer, the apoptotic cells are counted in the green channel. Figure 1 shows the results of this flow cytometry assay. We found that α-MSH 78% of the RAW cells are apoptotic when incubated in serum-free media overnight. We found a dose that α-MSH rescued macrophages in a concentration dependent manner. An optimal concentration of α-MSH at 10 ng/ml of a-MSH decreased the number of apoptotic cells to 18%. For the rest of the experiments in this project we will compare untreated RAW cells with RAW cells treated with 10 ng/ml α-MSH

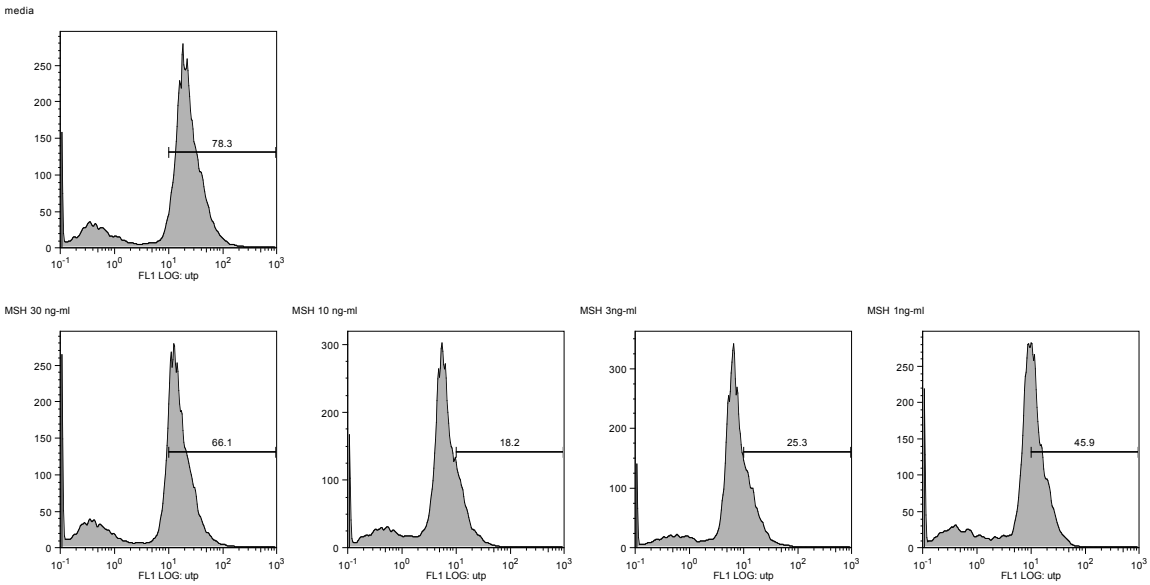

Figure 1. Treatment with alpha-MSH saves macrophages from apoptosis. The macrophages were incubated in serum-free media and treated with alpha-MSH (0 (media), 1, 3, 10, or 30 ng/ml). The cells were incubated overnight and then assayed for apoptosis by flow cytometry, using the Chemicon APO-DIRECT kit. Presented is the percentage of apoptotic cells..

We further examined the poteintial of α-MSH to suppress different apoptotic pathways The RAW cells were treated to induce a caspase independent apoptotic pathway with alpha-lactalbumin, and a reactive oxygen-dependent pathway with Sulfasalazine. The extrinsic caspase dependent pathway was induced by culturing the cells in serum-free media. The cells were incubated for 18 hours and assayed by immunoblotting of their lysate for BAX and Bcl-2 protein, and for Caspase 8 and Caspase 9 specific activity.

There was no observed α-MSH suppression of death in cells treated with alpha-lactalbumin, or with Sulfasalazine. Caspase 8 activity in RAW cells cultured in the serum-free media was suppressed by α–MSH in a dose-dependent manner along with the previously described decrease in TUNEL positive cells (Fig. 2). Under serum-free conditions, there was no change in Caspase 9 activity (Fig. 3), which was no different than in RAW cells under non-apoptotic serum containing conditions. While there is no detectible apoptosis under serum containing conditions a-MSH suppressed Caspase 9 activity (Fig. 4). In addition, RAW cells cultured in serum free media treated with α-MSH had a downward shift of about 20% in the ratio of BAX to Bcl-2 expression (Fig. 5), but little change in the ratio BAX to Bcl-2 expression in RAW cells under serum containing conditions (Fig. 6). Our next step is detect the possibility that α-MSH is inhibiting the expression of caspase 8 or inhibiting the cleavage of caspase 8 associated with its activation.

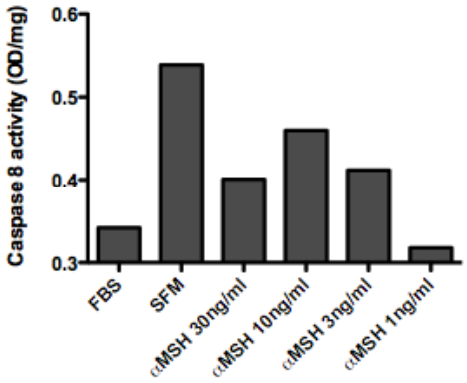

Figure 2. The effects of alpha-MSH on Caspase 8 activity in SFM-induced apoptosis. The macrophages were incubated in serum-free media and treated with alpha-MSH (0 (media), 1, 3, 10, or 30 ng/ml) or with 10%FBS. The cells were incubated overnight. Lysed and assayed for Caspase 8 activity using R&D Systems Caspase 8 colorimetric assay. Presented are the relative levels of OD/mg of lysate. The results show that under serum free conditions Caspase 8 activity is greatly augmented and there is a dose dependent alpha-MSH suppression of Caspase 8 activity in the macrophages under serum free conditions.

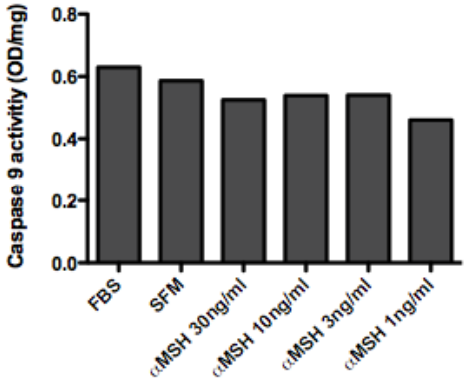

Figure 3. The effects of alpha-MSH on Caspase 9 activity in SFM-induced apoptosis. The macrophages were incubated in serum-free media and treated with alpha-MSH (0 (media), 1, 3, 10, or 30 ng/ml) or with 10%FBS. The cells were incubated overnight. Lysed and assayed for Caspase 9 activity using R&D Systems Caspase 9 colorimetric assay. Presented are the relative levels of OD/mg of lysate. The results show that under serum free conditions Caspase 9 activity is not augmented; however there is weak a dose response curve of alpha-MSH suppression of Caspase 9 activity in the macrophages under serum free conditions.

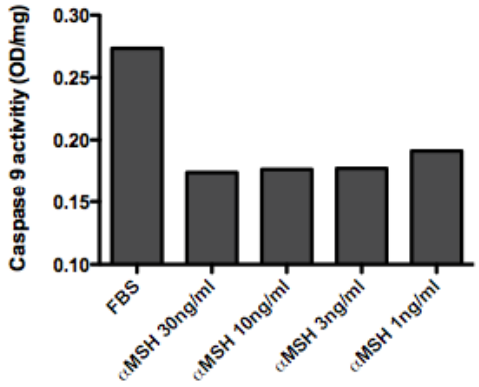

Figure 4. The effects of alpha-MSH on Caspase 9 activity in serum culture. The macrophages were incubated in media + 10% FBS and treated with alpha-MSH (0 (media), 1, 3, 10, or 30 ng/ml). The cells were incubated overnight, lysed and assayed for Caspase 9 activity using R&D Systems Caspase 9 colorimetric assay. Presented are the relative levels of OD/mg of lysate. The results show a strong alpha-MSH induced suppression of Caspase 9 activity in the macrophages under serum containing conditions.

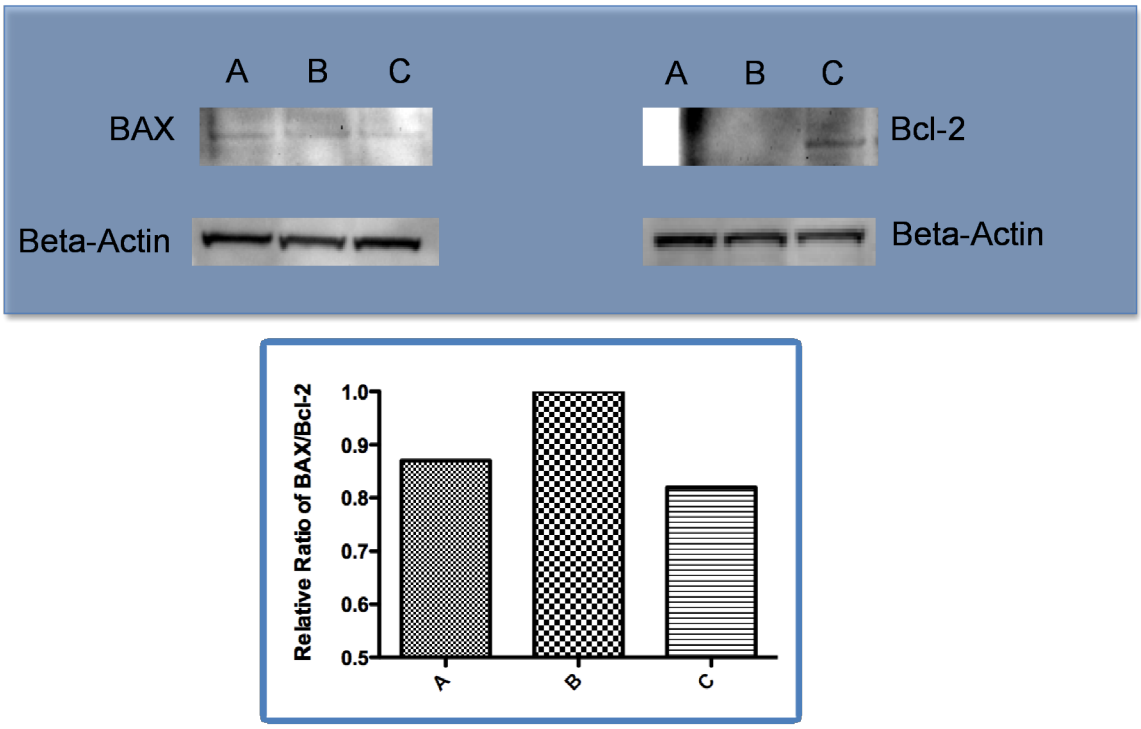

Figure 5. The effects of alpha-MSH on BAX and Bcl-2 levels in SFM-induced apoptosis. The macrophages were incubated in A) 10%FBS, B) serum-free media, and C) treated with alpha-MSH (10ng/ml) in serum-free media. The cells were incubated overnight. Lysed and immunoblotted for BAX, Bcl-2 and beta-Actin . Presented are representative of two experiments with similar results. The relative ratio of BAX to Bcl-2 was calculated using band density (Intensity/mm^2) of each band over its respective beta-actin band density. Higher Bax to Bcl-2 ratio are associated with induction of intrinsic apoptosis pathways.

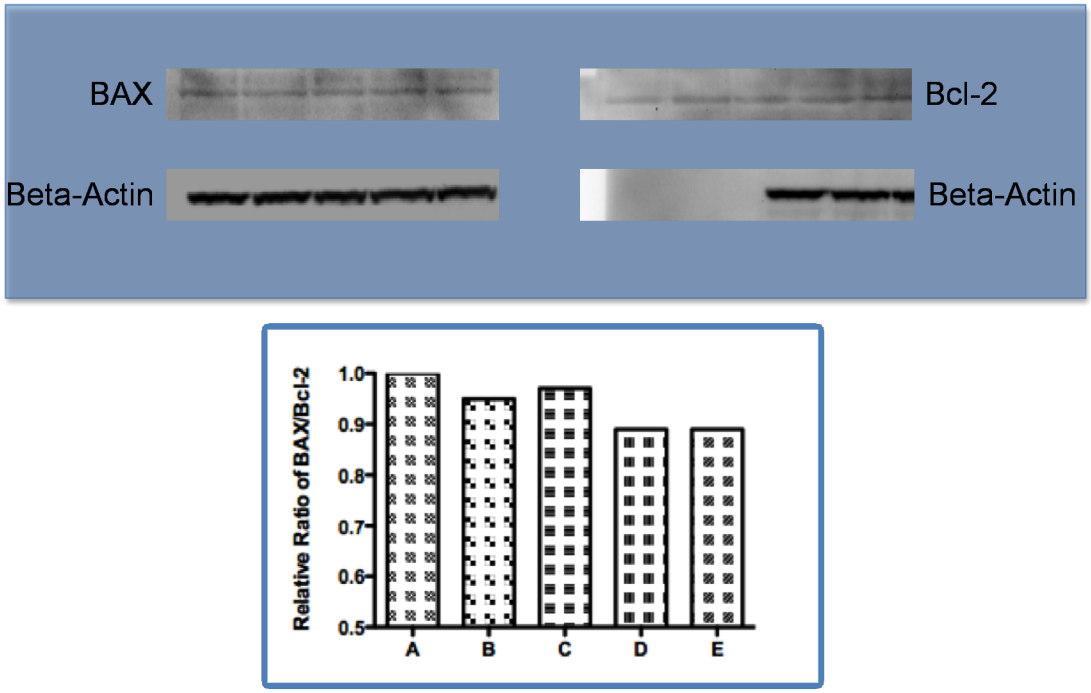

Figure 6. The effects of alpha-MSH on BAX and Bcl-2 levels in Serum-induced apoptosis. The macrophages were incubated in A) 10%FBS, or treated with with alpha-MSH B) 30 ng/ml, C) 10 ng/ml, D) 3 ng/ml, E) 1 ng/ml in serum-free media. The cells were incubated overnight. Lysed and immunoblotted for BAX, Bcl-2 and beta-Actin . Presented are the results of one experiment. The relative ratio of BAX to Bcl-2 was calculated using band density (Intensity/mm^2) of each band over its respective beta-actin band density.

KEY RESEARCH ACCOMPLISHMENTS:

- Under conditions that mimic the serum-free ocular retinal microenvironment macrophages activate caspase 8 activity and go into apoptosis.
- α-MSH rescues RAW cells from apoptosis induced by serum-free culture conditions
- α-MSH suppresses the activation of caspase 8 activity.
- α-MSH suppresses constitutive levels of caspase 9 activity.
- α-MSH activity is limited to caspase-dependent apoptosis pathways.

REPORTABLE OUTCOMES:

The current results were submitted as an abstract for ARVO 2010:
Natural Emergence of Regulatory Immunity in EAU
D.J. Lee[1,2]*, A.W. Taylor*[1,2]. [1]Schepens Eye Research Institute, Boston, MA; [2]Department of Opthamology, Harvard Medical School, Boston, MA.

CONCLUSION:

These results demonstrate that under the same serum-free conditions of our original observation of RPE modulation of macrophage activity α-MSH suppresses the activated extrinsic apoptotic pathway. The implications of these results are that applications of a-MSH may not only rescue macrophages/microglial cells with immunosuppressive properties but also suppress non-apoptotic caspase activities.

Task 9
Bruce R. Ksander, Ph.D.
Title: Glial Regulation of Neuronal Damage After Traumatic Brain Injury
Determine if secondary neuronal damage that occurs after a traumatic brain injury is caused when microglia produce neurotoxic soluble FasL. These studies will utilize a unique mutant knock-in mouse that produces membrane FasL (sFasL), but is unable to produce soluble FasL (sFasL). This is the first time this type of FasL knock-in mutation has been successfully produced.

Introduction:
Evidence indicates that the majority of neuronal loss that occurs after a traumatic brain injury is *not* caused by the acute phase injury, but occurs over a prolonged period of time after the injury (secondary damage). However, the mechanism of secondary neuronal damage remains unclear. Brain injury research to date has focused primarily on the pathophysiology of injured neurons with much less attention paid to non-neuronal cells. In the past decade, exciting discoveries have led to a reinterpretation of the role of glial cells, including astrocytes and microglia, in central nervous system (CNS) biology and pathology. Compelling evidence reveals that glial cells are adversely affected by trauma and that changes in the functions of these cells affect the fate of neurons after a traumatic brain injury.

Fas Ligand and microglia contribute to CNS injury- FasL is a 40 kDa type II transmembrane protein of the tumor neurosis factor (TNF) family that induces apoptotic cell death in susceptible cells expressing the Fas receptor. Recent data from our laboratory, and others, indicate that both Fas and FasL are up regulated after a traumatic brain injury and are likely to be involved in neuronal damage following injuries.

It has been shown that the Fas/FasL system is critical in the development of secondary damage induced by spinal cord injury. In an impressive series of experiments, Martin-Villalba and co-workers demonstrated that blocking the activity of CD95L (Fas Ligand) by treating mice with neutralizing antibodies within hours after a spinal cord injury *decreased* apoptosis at the injury site and *increased* neuronal survival. Moreover, they observed that blocking this pathway increased (i) axonal regeneration and (ii) functional recovery from the injury. An important point for our research is that the source of FasL and exact mechanism by which blocking FasL prevents neuronal damage and increases the recovery was not determined in these studies. We predict that the form of FasL produced will determine the function.

FasL can exist as either a membrane-bound (mFasL), or soluble protein (sFasL), each exhibiting opposing effects on inflammation and apoptosis. Following a traumatic brain injury, FasL is expressed by neutrophils, activated T cells, microglia, astrocytes, and neurons. Although microglia constitutively express FasL, they only release the soluble form of FasL (sFasL) after being activated or stimulated by mGlu2 (group II metabotropic glutamate receptor). A series of *in vitro* experiments by Jennifer Pocock and co-workers provided important clues as to how FasL might function *in vivo* following spinal cord injuries. They discovered that activated microglia release sFasL that induces neuronal apoptosis, a critical event associated with reactive gliosis.

However, it has not been possible, until our current study, to study the function of soluble or membrane FasL *in vivo*, since it was impossible to separate these two forms of FasL. The successful construction of our FasL knock-in mutant mouse made these important studies possible.

Based on our observations obtained on the form and function of FasL in the eye, we propose that secondary neuronal damage following a traumatic brain injury is caused when activated microglia produce soluble neurotoxic sFasL. Therefore, blocking the activation of microglia and/or the production of sFasL should reduce secondary neuronal damage and benefit patients with traumatic brain injuries.

Hypothesis:
This project will use a unique mutant mouse model to test the hypothesis that activated microglia produce neurotoxic soluble FasL that triggers apoptosis of Fas receptor positive neurons.

Technical Objectives / Specific Aims:

Subtask 9.1- Determine whether a traumatic brain injury that occurs in the absence of sFasL results in reduced neurotoxicity, and increased neuronal survival;

Subtask 9.2- Demonstrate that microglia are responsible for the reduced neurotoxicity.

Body:
We completed our work on subtask 9.1 and partially completed work on subtask 9.2.

Subtask 9.1- The membrane-only FasL knock-in mice (***ΔCS.1 mice***) were constructed and we demonstrated these mice were unable to cleave mFasL to produce the soluble form. There experiments utilized lymphocytes from WT and ΔCS.1 mice that were analyzed via Western blot and flow cytometry for the presence of mFasL and sFasL. These mice were used with the controlled cortical impact model of traumatic brain injury to determine the effect of the failure to cleave FasL on secondary neuronal damage. Our results indicated that secondary damage (as assessed by development of gliosis) was reduced 7 days after the traumatic brain injury, as compared with WT mice. Unexpectedly, the initial acute phase (day 2 after injury), appeared worse in ΔCS.1 mice. We interpret these results as indicating that either the presence of mFasL triggers a more dramatic acute inflammatory response quickly after the initial injury. However, in the absence of sFasL, this acute response rapidly subsides, resulting in less secondary neuronal damage. This interpretation will be tested in future experiments.

Subtask 9.2- This subtask required that we immortalize brain microglia from ΔCS.1 mice. While we used a procedure that previously had been successful for immortalizing microglia from the brain of WT mice, our effectors were initially unsuccessful. This was done with the assistance of Dr. Golenbock (Dept of Microbiology & Immunology, Univ of Mass Medical School) who had previously used the J2 retrovirus to immortalize brain microglia from B6 wild-type mice. It was unclear why these experiments initially failed, but it was likely due to the retrovial preparation, since we were successful after making a new preparation of the J2 retrovirus. These cells were analyzed for: morphology,

phenotype, and cells surface markers. These data demonstrated that we had immortalized brain microglia from ΔCS.1 mice. We are now able to continue with the experiments in subtask 9.2.

Key research accomplishments:

Subtask 9.1- Demonstrated that secondary damage following a traumatic brain injury is reduced in mice that fail to cleave Fas Ligand.

Subtask 9.2- Isolated and immortalized brain microglia from wild-type and ΔCS.1 mice. These cells can now be used to study the protective mechanisms associated with the reduced secondary damage observed in subtask 9.1.

Reportable outcomes:
We are currently working on a paper to report our results.

Conclusions:
Following a traumatic brain injury, the amount of secondary damage is reduced in the absence of soluble FasL. These results imply that sFasL is neurotoxic and prevents the rapid healing of traumatic brain injuries.

Task 10
Peter Bex, Ph.D.
Sources of Visual Impairment following Mild Traumatic Brain Injury
After numerous unsuccessful efforts to locate veterans with mild traumatic brain injury, regrettably the project has been terminated due to the unavailability of study subjects.

Task 11
Andrius Kazlauskas, Ph.D.
Title: The Role of Vitreal Factors in Determining the Severity of Proliferative Vitreoretinopathy

INTRODUCTION:
PVR is a serious problem in patients with retinal detachments (Campochiaro, 1997; Committee, 1983; Michels et al., 1990; Pastor, 1998). It is characterized by the formation of a fibroproliferative membrane that contracts and tears the retina from the back of the eye. PVR occurs in 5-10% of the patients who undergo retinal reattachment surgery. Of this group, nearly 20-40% have recurring episodes of PVR and partial vision loss. Military personnel that survive violent traumatic episodes are prone to severe PVR that has a particularly poor prognosis. Aside from surgical interventions to relieve the vitreoretinal traction, there are no treatment options. Thus there is an acute need for pharmacological/molecular-based therapies for PVR.

BODY:
We recently discovered that while vitreous from rabbits or patients with PVR had readily detectable levels of platelet-derived growth factor (PDGF) (Lei et al., 2007), the vitreous activated PDGF receptor alpha (PDGFRα) poorly (Lei et al., 2009). Furthermore, the

PDGF present in rabbit vitreous underperformed because a heat-labile agent suppressed PDGF-dependent activation of PDGFRα. Furthermore, this heat-labile inhibitor appeared to be acting at the level of PDGFRα.

In light of the detailed reports that were submitted for each of the first 3 quarters, I am including only a brief summary for these periods. For the fourth quarter, a detailed description is provided.

First Quarter

- The inhibitory activity present in vitreous appears to associate with the extracellular domain of PDGFRα
- Galectin 3 was identified by mass spec as one of the vitreal proteins that bound to the extracellular domain of PDGFRα
- Recombinant galectin 3 did not prevent PDGF from activating PDGFRα, and is therefore not likely to be the inhibitor present in the vitreous.

Second Quarter

- The inhibitory activity present in the vitreous of rabbits with PVR was also present in the vitreous isolated from patients with PVR.

Third Quarter

- We completed the characterization of the PDGF/PDGFR inhibitory activity that is present in vitreous of patients with PVR.

Fourth Quarter

In the fourth quarter we identified one component of the inhibitory activity present in vitreous of patients and rabbits with PVR.

Modification of the Inhibitor-Purification Strategy

We previously identified an affinity matrix (TRAP, which is a PDGFRα extracellular domain-Fc fusion protein) that appeared to capture the inhibitory activity that was present in the vitreous. The approach that we originally used to elute proteins recovered with the TRAP released both the eluted proteins and the TRAP itself. This created a major problem because TRAP was present at such a high concentration that it precluded identification of at least some of the proteins that were recovered from the vitreous. To overcome this hurdle we reduced that amount of TRAP and chemically crosslinked it to protein A sepharose beads. These two modifications prevented it from contaminating the sample during the elution step (Fig 1a). Chemically crosslinking the TRAP did not compromise its function; it retained full ability to remove inhibitory activity from PVR vitreous and neutralize PDGFs (Fig 1b).

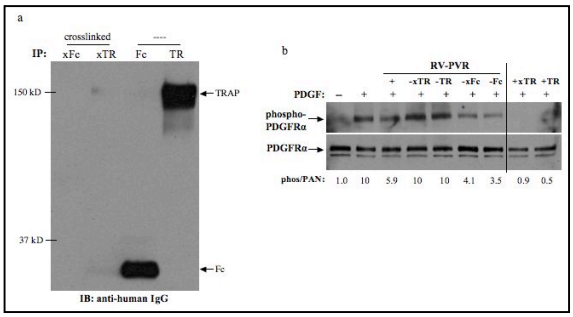

Figure 1. Characterization of chemically crosslinked TRAP (a) TRAP (TR) or control IgG-Fc fragment (Fc) was or was not crosslinked to Proteins A sepharose beads and then used to recover proteins from equal volumes of PVR rabbit vitreous. The samples were washed, the proteins were eluted and subjected to Western blot analysis using an anti-human IgG antibody. **(b)** Serum-starved ARPE-19α cells were treated for 10 min

with the indicated agents, lysed and total cell lysates were subjected to anti-phospho-PDGFRα (pTyr720) and anti-panPDGFRα western blot analysis. The signal intesity was quantified by densitometry, normalized to total (pan) PDGFR and expressed as a fold increase relative to unstimulated cells.

An additional change that we instituted in our second attempt to purify the inhibitor present in vitreous was to submit all recovered proteins to mass spec analysis instead of resolving them by SDS-PAGE and pre-selecting proteins on the basis of their molecular mass/abundance.

Results from mass spec Analysis

The chemically crosslinked TRAP was incubated with rabbit PVR vitreous, washed, the retained proteins were eluted, digested with trypsin and subjected to mass spec analysis. Comparing the data sets from control and experimental groups indicated that approximately 20 proteins were specifically recovered with TRAP. Of these we chose to focus on VEGF-A as a potential inhibitor of PDGF because VEGF has a similar structure to PDGF (Muller et al., 1997) and can bind to PDGFR (Ball et al., 2007).

VEGF is present in the vitreous and binds to TRAP

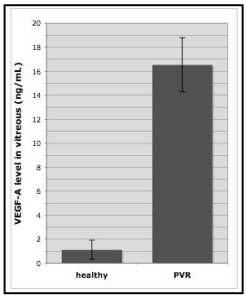

Multiplex analysis confirmed that VEGF was present in the vitreous (Fig 2). Comparison of vitreous from healthy and PVR rabbits indicated that the level of VEGF increased as rabbits developed PVR (Fig 2), which is consistent with our previous observation that there was more inhibitory activity in PVR vitreous as compared with healthy controls (data not shown). Moreover, TRAP recovered VEGF from PVR vitreous, whereas the negative controls were much less effective (Fig 3). Finally, like the inhibitory activity, VEGF-A was heat labile (data not shown).

Figure 2. VEGF-A in vitreous of healthy and PVR rabbits. Vitreous from healthy or PVR rabbits was subjected to multiplex analysis. The results for VEGF-A (ng/ml) are presented; the mean +/- sd is presented; n = 7 and 10 for healthy and PVR vitreous, respectively.

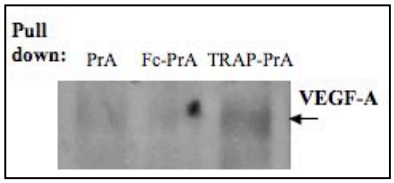

Figure 3. VEGF-A was recoverable with TRAP from rabbit PVR vitreous. Protein A agarose (PrA), PrA loaded with either the Fc fragment of IgG (Fc-PrA), or TRAP (TRAP-PrA) was incubated with PVR rabbit vitreous, washed and the recovered proteins were subjected to an anti-VEGF-A Western blot analysis.

VEGF bound to PDGFRα and prevented its activation by PDGF

The finding that TRAP recovered VEGF from PVR vitreous suggests that VEGF is able bind to PDGFRα, an idea that was supported by work from another group using a

different cell type (Ball et al., 2007). Our experiments with human RPE cells confirmed the idea that VEGF could bind PDGFRα and promote its dimerization (Fig 4).

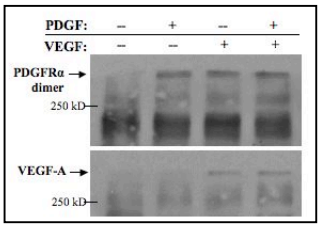

Figure 4. VEGF-A interacted with PDGFRα. Serum-starved ARPE-19α cells were cooled on ice and allowed to bind PDGF-A (10 ng/ml) and/or VEGF-A (20 ng/ml), crosslinked and then immunoprecipitated with an anti-PDGFRα antibody. Immunoprecipitated proteins were subjected first to anti-PDGFRα and then anti-VEGF-A western blot analysis. The anti-PDGFR/VEGF bands detected above 250 kD represent the ligand (PDGF/VEGF)-bound PDGFRα dimer.

Finally, we tested if VEGF was capable of preventing PDGF-dependent activation of PDGFRα. We found that this was indeed the case (Fig 5). Stimulating cells with PDGF when VEGF was also present reduced the extent of PDGFRα activation to 27% of what was observed in the absence of VEGF. Despite the fact that VEGF induced dimerization of PDGFRα, it was unable to effectively activate it, perhaps because the nature of the dimer that formed was not functional, i.e. did not promote a conformation change in the receptor's kinase domain that promoted catalysis.

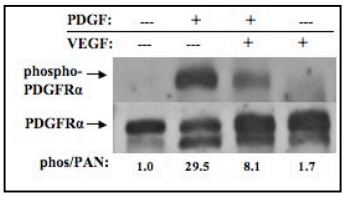

Figure 5. VEGF attenuated PDGF-dependent activation of PDGFRα. Serum-starved ARPE-19α cells were treated with buffer alone or various combinations of PDGF-A (10 ng/ml) and VEGF-A (20 ng/ml) for 10 min. Following treatment, cells were lysed and subjected first to anti-phospho-PDGFRα (pTyr720) and then anti-panPDGFRα western blot analysis. Immunoblot bands were quantified, normalized to total PDGFR; the values at the bottom of the panel are the fold increase in PDGFRα phosphorylation over unstimulated control.

KEY RESEARCH ACCOMPLISHMENTS:

- Identification of VEGF as one of the vitreal agents that was capable of attenuating PDGF-dependent activation of PDGFRα.

REPORTABLE OUTCOMES:

None.

CONCLUSION:

We identified one of the agents (VEGF-A) in PVR vitreous that attenuated PDGF-dependent activation of PDGFRα. The existence of many reagents to detect VEGF-A and modulate VEGF-A-dependent action will accelerate translation of this discovery into new therapeutic approaches to manage the risk of PVR. Additional studies to learn whether VEGF-A is the primary inhibitory agent present in vitreous, and if it functions to promote or inhibit PVR are key questions to address in future studies.

REFERENCES:

Ball, S.G., Shuttleworth, C.A., and Kielty, C.M. (2007). Vascular endothelial growth factor can signal through platelet-derived growth factor receptors. J Cell Biol *177*, 489-500.

Campochiaro, P.A. (1997). Mechanisms in ophthalmic disease: Pathogenic mechanisms in proliferative vitreoretinopathy. Arch Ophthalmol *115*, 237-241.

Committee, T.R.S.T. (1983). The classification of retinal detachment with proliferative vitreoretinopathy. Ophthalmology *90*, 121-125.

Lei, H., Hovland, P., Velez, G., Haran, A., Gilbertson, D., Hirose, T., and Kazlauskas, A. (2007). A potential role for PDGF-C in experimental and clinical proliferative vitreoretinopathy. Invest Ophthalmol Vis Sci *48*, 2335-2342.

Lei, H., Velez, G., Hovland, P., Hirose, T., Gilbertson, D., and Kazlauskas, A. (2009). Growth factors outside the PDGF family drive experimental PVR. Invest Ophthalmol Vis Sci *50*, 3394-3403.

Michels, R.G., Wilkinson, C.P., and Rice, T.A. (1990). Proliferative retinopathy (St. Louis, Mosby).

Muller, Y.A., Christinger, H.W., Keyt, B.A., and de Vos, A.M. (1997). The crystal structure of vascular endothelial growth factor (VEGF) refined to 1.93 A resolution: multiple copy flexibility and receptor binding. Structure *5*, 1325-1338.

Pastor, J.C. (1998). Proliferative vitreoretinopathy: an overview. Surv Ophthalmol *43*, 3-18.